

PROPULSIVE PERFORMANCE OF A C_3H_4/H_2O_2 ROCKET PROTOTYPE FOR FUTURE GREEN BI-PROPELLANT THRUSTERS

Angelo Pasini

SITAEL S.p.A.

PhD, Project Manager - Chemical Propulsion

5 Via A. Gherardesca, 56121, Ospedaletto, Pisa, Italy

a.pasini@alta-space.com

Giovanni Pace (SITAEL S.p.A., g.pace@alta-space.com), Lucio Torre (SITAEL S.p.A., l.torre@alta-space.com)

ABSTRACT

In the framework of the PulCheR project, an experimental test campaign on a 40 N bipropellant thruster prototype has been carried out with the aim of assessing the attainable propulsive performance in steady state conditions of 98% concentration hydrogen peroxide and propyne. The preliminary atmospheric tests without the combustion chamber on the selected liquid/liquid coaxial injectors show the lack of the hypergolicity of the innovative propellant combination when injected in liquid phase at ambient temperature and the ignitability of the mixture when the decomposition of propyne is promoted by a spark plug. In the final tests on the bipropellant prototype, the tested ignition device has not been able to start the combustion and, therefore, the experimental propulsive performance has not been assessed.

NOMENCLATURE

A	= area
C_d	= discharge coefficient
C_F	= thrust coefficient
c^*	= characteristic velocity
D, d	= diameter
F	= thrust
g	= gravitational acceleration at sea level
I_{sp}	= specific impulse
\dot{m}	= mass flow rate
O/F	= oxidizer/fuel mass ratio
p	= pressure
R	= gas constant of the exhaust gases
Re	= Reynolds number
T	= temperature
v	= velocity
We	= Weber number
α	= conical half angle
μ	= dynamic viscosity
σ	= surface tension
γ	= specific heat ratio of the exhaust gases
η_{c^*}	= characteristic velocity efficiency (c_{exp}^*/c_{theo}^*)
η_{CF}	= thrust coefficient efficiency ($C_{F,exp}/C_{F,theo}$)
$\eta_{\Delta T}$	= temperature efficiency ($(T_{exp}-T_{amb})/(T_{ad}-T_{amb})$)

Subscript

ad	= adiabatic reaction (decomposition/combustion)
amb	= ambient
b	= bore
C, CC	= combustion chamber

<i>e</i>	= exit
<i>exp</i>	= experimental
<i>FUEL</i>	= fuel
<i>i</i>	= inner, injector
<i>o</i>	= outer
<i>OXID</i>	= fuel
<i>t</i>	= throat
<i>theo</i>	= theoretical

Acronyms

CV	= Cavitating Venturi
ECHA	= European Chemicals Agency
F	= Fuel
FM	= FlowMeter
GPRTF	= Green Propellant Rocket Test Facility (SITAEL S.p.A.)
HTP	= High Test Peroxide
LC	= Load Cell
LPG	= Liquefied Petroleum Gas
O	= Oxidizer
REACH	= Registration, Evaluation, Authorisation and Restriction of Chemicals
SVHC	= Substances of Very High Concern
TC	= Thermocouple

1 INTRODUCTION

PulCheR (Pulsed Chemical Rocket with Green High Performance Propellants)[1-3] is a R&D project funded by the European Union Seventh Framework Programme (FP7/2007-2013) under grant agreement n°313271. The two main goals of the project are the demonstration of the feasibility of a new propulsion concept and the identification of high performance green propellants for powering future mono and bipropellant thrusters exploiting both the conventional propulsion concept and the new one proposed by the project.

The defence mechanism of a notable insect, the bombardier beetle,[4-6] has inspired the new propulsion concept. When assaulted, the bombardier beetle squirts a hot mixture of chemical liquids out if its rear end obtained by the reaction of two chemicals, hydroquinones and hydrogen peroxide, with a mixture of catalase and peroxidases dissolved in water. The flow of reactants into the reaction chamber and subsequent ejection to the atmosphere occurs cyclically at a rate of about 500 times per second and with the total pulsation period lasting for only a fraction of a second. In the new propulsion concept, the propellants are fed in the combustion chamber at low pressure and the thrust is generated by means of high frequency pulses. The radical innovation introduced by this concept is the elimination of any external pressurizing system even if the thruster works at high pressure inside the combustion chamber. At each pulse, pressurization of the combustion chamber gases takes place due to the decomposition or combustion reaction, and the final pressure is much higher than the one at which the propellants are stored. The pulsed chemical rocket concept is potentially able to substitute many currently used propulsion systems for accessing space.[7,8] The feasibility of this new propulsion concept is currently under investigation at breadboard level in both mono and bipropellant configurations.

The identification and the experimental investigation of green propellants with potential similar performance to the current state-of-the-art for monopropellant and bipropellant thrusters are nowadays of particular interest.[9-10] In fact, the recent inclusion of hydrazine into the Candidate List of Substances of Very High Concern (SVHC),[11] in accordance with the REACH (Registration, Evaluation, Authorisation and Restriction of Chemicals) regulation, by the European Chemical Agency

(with the consequent phasing-out for non essential use foreseen in mid 2017 at earliest [12]) has renewed the interest towards the so called “green” propellants.[13,14]

Moreover, the use of non-toxic “green” propellants is attractive also in view of the economic benefits, especially connected with the substantial cost saving in manufacturing and ground operating of spacecraft, because the handling of toxic propellants requires expensive safety measures, dedicated special precautions and specific infrastructure provision.[15]

The substitution of hydrazine is dramatically critical for monopropellant thrusters but it also affects the choice of the propellants for the bipropellant engine since, later or soon, also its by-products will be likely phased-out. The hunting of high performance green propellant combination for bipropellant thrusters is particularly tough since the current bipropellant propulsion systems require both the steady state and the pulse mode operations that can be easily obtained only with hypergolic propellants.

The present paper reports the experimental results attained on a rocket bipropellant prototype specifically designed for exploring the stationary (not-pulsed) propulsive performance of the green propellant combination of propyne and hydrogen peroxide. The main aim of the experimental characterization of the propulsive performance in steady state condition is the identification of a reference value for assessing the propulsive performance of the new propulsion concept proposed in the PulCheR project. The test campaign has been carried out in SITAEL’s Green Propellant Rocket Test Facility.

2 TEST APPARATUS

2.1 Bipropellant Thruster Prototype Design Features

In the framework of the PulCheR project, a bipropellant thruster prototype has been designed with the main aim of assessing the experimental steady state propulsive performance of the innovative propellant combination composed by Hydrogen Peroxide (98% by weight) and Propyne (99% by weight). The theoretical adiabatic flame temperature and the corresponding theoretical characteristic velocity of the combustion products of hydrogen peroxide and propyne as a function of the oxidizer/fuel mass ratio for different H_2O_2 concentration are reported in Figure 1. The resulting theoretical specific impulse in vacuum and at sea level expected for the nominal design of the thruster demonstrator are shown in Figure 2. The design features of the bipropellant thruster prototype are reported in Table 1.

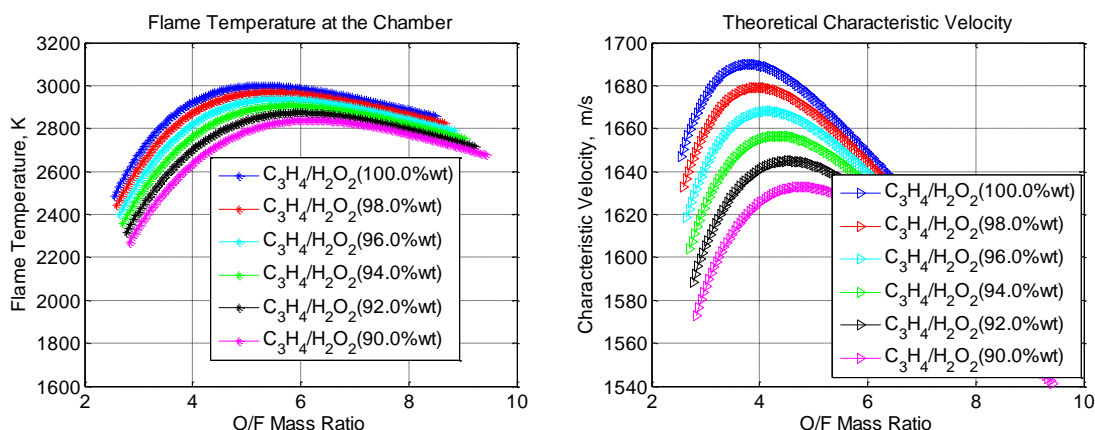


Figure 1. Adiabatic flame temperature (left) and characteristic velocity (right) of the combustion products of hydrogen peroxide and propyne as a function of the oxidizer/fuel mass ratio for different H_2O_2 concentration.

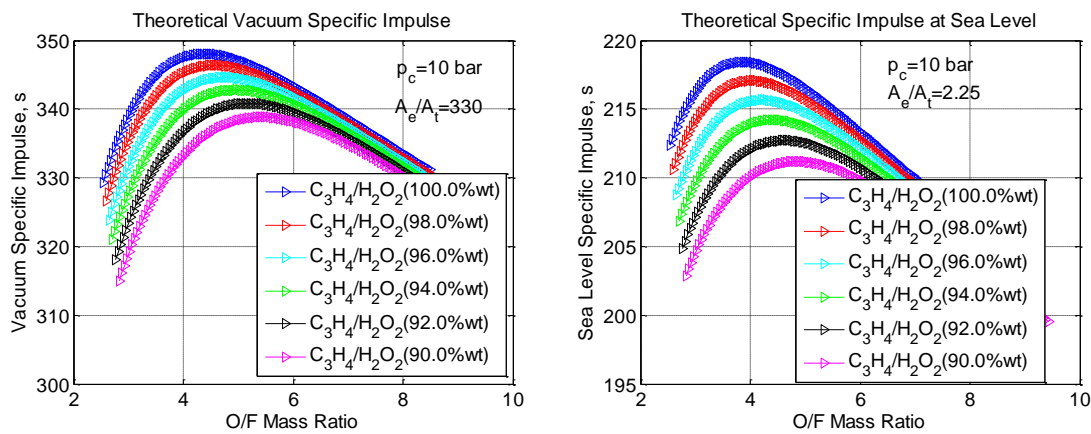


Figure 2. Theoretical specific impulse in vacuum (left) and at sea level (right) of the combustion products of hydrogen peroxide and propyne as a function of the oxidizer/fuel mass ratio for different H_2O_2 concentration.

Bipropellant Thruster Prototype Nominal Design	
Propellants	$C_3H_4/H_2O_2(98\%)$
Nominal Mixture Ratio	4.76
Nominal Chamber Pressure	10 bar
Nominal Vacuum Thrust	40 N
Bell-Shaped Nozzle Expansion Ratio for Vacuum	330
Conical Nozzle Expansion Ratio for Atmospheric Test ($D_t = 5 \text{ mm}$; $D_e = 7.5 \text{ mm}$; $\alpha = 15^\circ$)	2.25

Table 1. Main features of the bipropellant thruster prototype.

The main parameters which have driven the geometry and materials choice have been the nominal chamber pressure (p_G about 10 bar) and the adiabatic combustion temperature expected for the combination of these propellants (T_G about 2950 K). Two materials have been chosen for the combustion chamber: TZM (titanium-zirconium-molybdenum) and Silicon Nitride which show very interesting physical, mechanical and thermal properties. The melting point for both the materials is very near to the adiabatic flame temperature or even lower, as in the case of TZM. This aspect is a critical issue for the firing time of the thruster which is very limited by the high convective heat transfer coefficient which results in the converging part of the nozzle near the throat. Indeed some preliminary calculations have been carried out based on a simplified model of the combustion chamber. As a results, it came out that the firing time of the thrusters will have to be limited to a few seconds, which is anyway enough to set a steady state condition in the combustion chamber, given that the flow residence time is lower than 10 ms.

Due to the lack of experimental results concerning the hypergolicity of the propellants, the prototype has been designed in order to be capable of performing tests both with hypergolic propellants and with propellants that must be ignited by means of suitable devices such as a spark plug or a catalytic bed. The main components of the prototype are shown in Figure 3. With the exception of the combustion chamber and the coaxial injector, the other components of the bipropellant thruster have been made of a particular stainless steel (AISI 310S) which ensures a high mechanical resistance at high temperature.

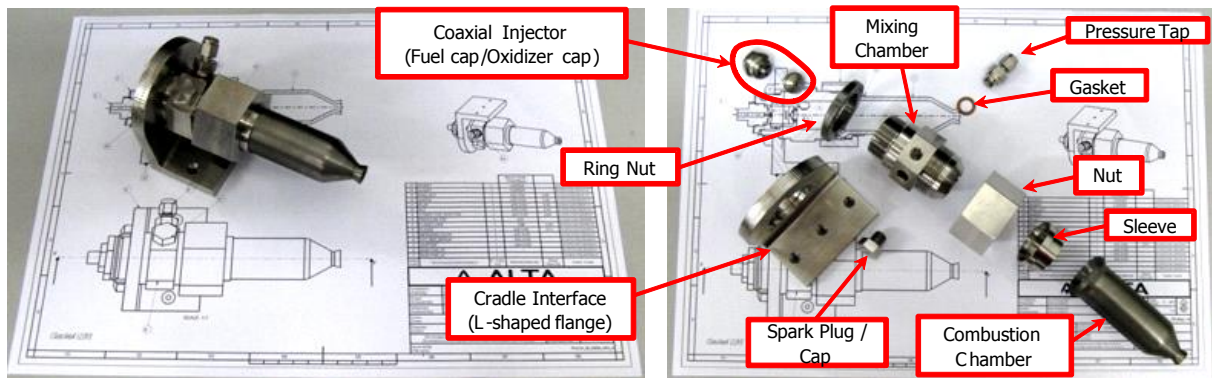


Figure 3. Main components of the bipropellant thruster prototype.

The mixing chamber, visible in Figure 4, is the core of the bipropellant prototype and it is interfaced with the combustion chamber, the propellants injector and the L-shaped flange of the cradle.

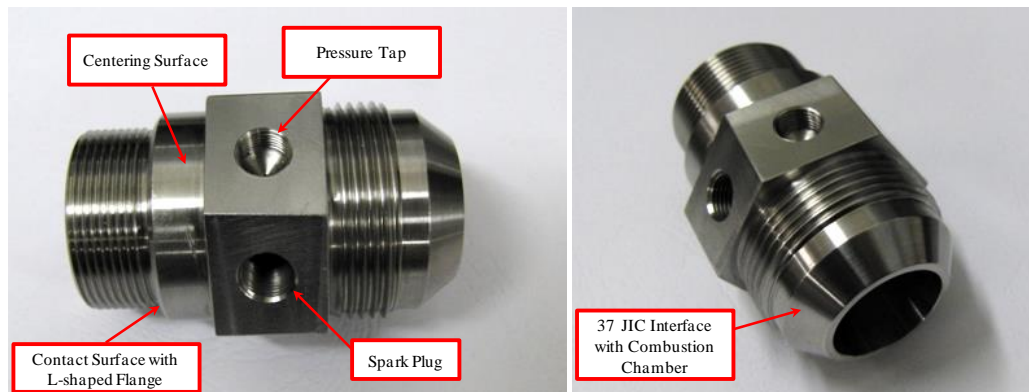


Figure 4. The mixing chamber of Alta's bipropellant prototype

The JIC 37° flare connection of the mixing chamber assures the possibility of interchanging the combustion chamber. The coaxial injector, made of stainless steel, is provided by Spraying System Co. and is made up of two components: a fuel cap and an air cap for the injection. Moreover, the air atomizing nozzles allow for two different mixing set-ups: the external mix set-up (see top of Figure 5) in which the propellants streams are mixed outside of the nozzle; the internal mix set-up in which the fluids are mixed internally to produce a completely atomized spray (see bottom of Figure 5).

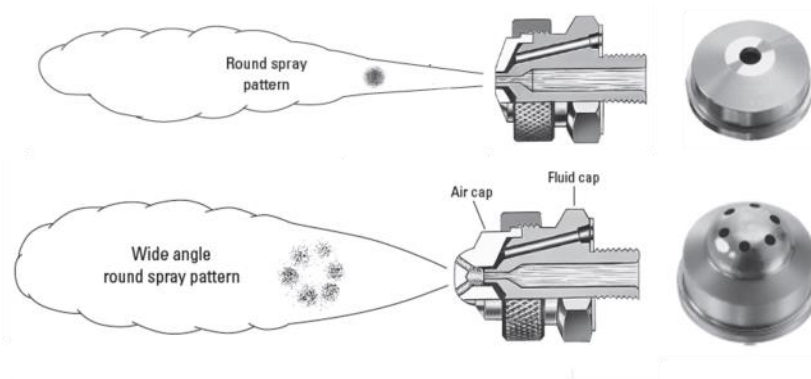


Figure 5. External mix set-up (top) and internal mix set-up (bottom).

The mixing chamber has a pressure tap used to check the pressure of the burnt mixture and a tap provided for possibly hosting a spark plug in order to burn the injected mixture. The selected spark plug is the NGK CMR6A which can easily replace the tap and guarantee the sealing by means of the integrated gasket. This spark plug is a compact (Bantam) type resistive plug (with resistance of about 10 k Ω) with a medium (6) heat rating number. A medium value for the heat rating number has been chosen given the gaseous flow temperature is not known a priori in the spark plug region. This choice has been made in order to avoid overheating of the spark plug during the operation (that would happen for low heat rating numbers) but, at the same time, to avoid the fouling of the spark plug (that would happen for high heat rating numbers).

Moreover, the mixing chamber has the capability of hosting a cartridge of a catalytic bed with a maximum length of 15 mm and a maximum volume of 2.5 cm³. Differently to the case of coaxial injector where HTP is injected liquid phase, the liquid HTP passes through a catalyst in order to decompose itself and thus producing a hot steam which could easily mix with flashing propyne.

The cradle interface is made of AISI 316L and it is L-shaped in order to host the thruster and rigidly connect it to the one-degree of freedom force balance. The flange has a groove where the mixing chamber is inserted so that its axis is aligned to the load cell and its axial placement is fixed by means of a ring nut.

2.2 Propulsive Performance Assessment: Test Facility and Instrumentation

The experimental campaign has been carried out in SITAEL's Green Propellant Rocket Test Facility (GPRTF), an easily reconfigurable and expandable experimental apparatus especially designed for performance characterization of small monopropellant (H₂O₂), [16-21] bipropellant (H₂O₂-hydrocarbon) and hybrid (H₂O₂-NfH₂) [22] rocket engine prototypes and catalytic reactors operating at thrust levels in the 1-40 N and 25-100 N ranges. The facility mainly comprises the propellants feed systems and the thrust balance.

Concerning the oxidizer supply system, all of the hydrogen peroxide lines and the main tank are made of AISI 316 stainless steel internally coated with Teflon. Hydrogen peroxide is stored in a 2.5 liters tank and is pressurized by gaseous Nitrogen. Its physical conditions are continuously monitored by means of a J-type thermocouple and a gauge pressure transducer. If the peroxide starts to decompose, the tank can be vented to the atmosphere by means of a remotely controlled valve or, in the absence of the operator, by the combination of a relief valve and a burst disc calibrated for opening at suitably spaced pressure values. The hydrogen peroxide mass flow rate is controlled by means of interchangeable cavitating venturis and it is monitored by a Coriolis flowmeter. The operation of the venturi is continuously monitored by a differential and a downstream pressure transducer.

The fuel feeding line mainly comprises the valves, relief valves, check valves, pressure transducers and thermocouple necessary for controlling the filling & drain processes and the injection of the fuel inside the thruster (see Figure 6). All the lines and the main tank for propyne are made of AISI 316 stainless steel which is compatible with this type of hydrocarbon. Propyne is stored in a 4.5 liters tank and is pressurized by gaseous Nitrogen. Its physical conditions are continuously monitored by means of a K-type thermocouple which directly measures the propyne temperature and a gauge pressure transducer. Given the possibility for propyne to decompose, the tank can be vented to the atmosphere by means of a remotely controlled valve in order to empty the nitrogen from the tank or, in the absence of the operator, by a relief valve calibrated for opening at suitable pressure value. The propyne mass flow rate is fixed by means of interchangeable cavitating venturi. The operation of the venturi can be continuously monitored by using two pressure transducers placed on each side of the venturi. Along the fuel firing line, before the cavitating venturi, is placed a turbine flow meter from Flow Technology. For this experimental campaign, both the venturis have been designed by FlowMaxx Engineering in order to provide the nominal mass flow rate at an inlet pressure of 35 bar. [23]

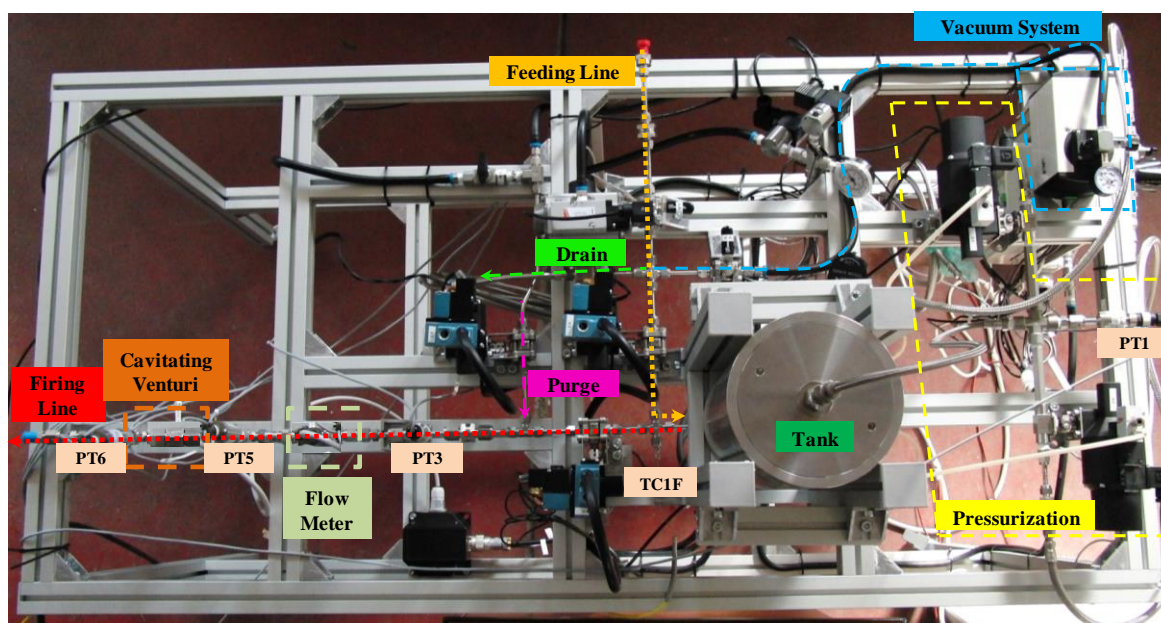


Figure 6. GPRTF fuel system.

The thruster is mounted on a one degree-of-freedom dynamometric force balance. In order to evaluate the performance of the thruster prototype and the following measurements are acquired:

- the chamber pressure, by means of an absolute pressure transducer mounted in recessed position for protection from the high temperatures;
- the injection pressure by means of two absolute pressure transducers (one per each propellant line) with the pressure taps just before the injector;
- the thrust, by means of a subminiature compression load cell.

Table 2 summarizes the model, the physical range, the accuracy and the location of all the transducers installed in the GPRTF and Figure 7 shows the sketch of the transducers arrangement used in the test campaign.

A DC source, capable of supplying different output voltages, provides the transducers with the required electric excitations. The data coming from the sensors and transducers installed in the facility are acquired and transferred to a personal computer by means of a National Instruments acquisition board, capable of acquiring 32 analogic channels and 48 digital channels at a maximum sampling rate of 1.25 MS/sec. The acquisition board is connected to different SCXI conditioning and filtering modules, also produced by National Instruments. A LabVIEW® data acquisition and control program is used for real time display of the data and for recording all of the acquired signals. A 20 Samples/s acquisition rate has been selected for compatibility with the maximum speed of the acquisition board and of the personal computer CPU, which represents the most stringent speed limitation of the present experimental configuration. Pressure, mass flow rate and thrust signals have been low-pass filtered by means of a 10 Hz cut-off frequency analog Butterworth filter. A lower cut-off frequency (4 Hz) has been used for the temperature signals.

	Transducer (Model)	Range	Accuracy	Location
Oxidizer Supply Facility	Thermocouple J-type (6 mm OD, mineral-insulated, by Watlow)	-40 – 750 °C	± 1.5 °C (≤375 °C)	main tank (TC10)
	gauge pressure transducer (PTU60 model, by Swagelok)	0–60 bar	± 0.43% FSO	main tank (PT10)
	differential pressure transducer (FP2000 model, by Honeywell)	0–500 psi	± 0.1% FSO	across the venture (PT20)
	gauge pressure transducer (PTU40 model, by Swagelok)	0–40 bar	± 0.43% FSO	downstream of the Venturi (PT30)
	Coriolis mass flow meter (MFS 7100 S04 model, by Krohne)	0–100 kg/h	± 0.1% measured value	downstream of the Venturi (FMF)
	absolute pressure transducer (Honeywell FP2000)	0–51 bar	± 0.1% FSO	firing line (downstream of flowmeter) (PT6)
Fuel Supply Facility	Thermocouple K-type (1 mm OD)	-200 – 1350°C	± 1.5 °C (≤375 °C) ± 0.004 °C (≤1000 °C) ± 4 °C (>1000 °C)	firing line (TC1F)
	gauge pressure transducer single end (PTU40 model, by Swagelok)	0–40 bar	± 0.5% span	main tank (gas side) (PT1)
	gauge pressure transducer through flow (PTU40 model, by Swagelok)	0–40 bar	± 0.5% span	firing line (upstream of Venturi) (PT3)
	absolute pressure transducer (Honeywell FP2000)	0–51 bar	± 0.1% FSO	firing line (upstream of flowmeter) (PT5)
	Turbine mass flow meter (FT4-6AEYWULEA-1 FT model, by Flow Technology)	0.11–11 lpm	± 0.05% measured value	firing line (downstream of Venturi) (FMF)
	absolute pressure transducer (Honeywell FP2000)	0–51 bar	± 0.1% FSO	firing line (downstream of flowmeter) (PT6)
Test Section	gauge pressure transducer (PTU60 model, by Swagelok)	0–60 bar	± 0.43% FSO	upstream the oxidizer injector (PT40)
	gauge pressure transducer (PTU60 model, by Swagelok)	0–60 bar	± 0.43% FSO	upstream the fuel injector (PT4F)
	absolute pressure transducer (XTM-190M-35BAR A, by Kulite)	0–35 bar	± 0.1% FSO	combustion chamber (PTCC)
	load cell (model 13 by Sensotec)	10 lbm	± 0.9% FSO	on the cradle (LC)

Table 2. GPRTF sensors list.

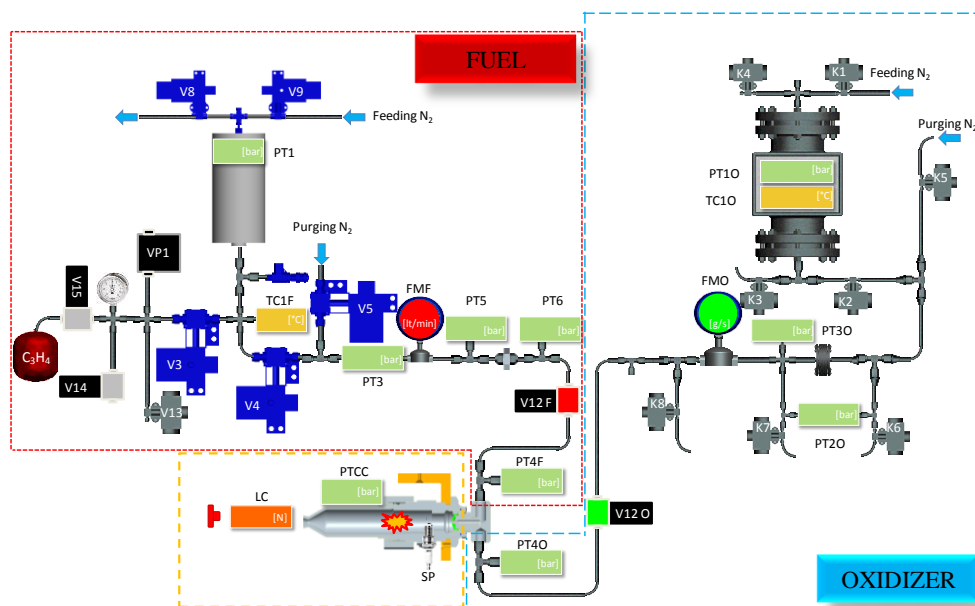


Figure 7. Arrangement of the transducers for the test campaign.

The test facility has been instrumented in such a way that the most important propulsive parameters for bipropellant thrusters (such as the specific impulse, the thrust coefficient and the characteristic velocity) can be experimentally measured. In fact, the specific impulse, defined as

$$I_{sp} = \frac{F}{mg} = \frac{C_F c^*}{g}$$

can be experimentally obtained from the measurements of the load cell and the flowmeters. Since the specific impulse strongly depends on the ambient conditions, the experimental results obtained at sea level must be scaled to extrapolate the propulsive performance in vacuum. As long as the throat is choked, the parameter that is mainly affected by the ambient conditions is the thrust coefficient, C_F . Its theoretical value depends only on the properties of the exhausted gases, the expansion area ratio and the ratio between the ambient and the combustion chamber pressure. During the experiments, the actual value of the thrust coefficient can be easily obtained from the chamber pressure and thrust measurements. The thrust coefficient efficiency is the ratio between its actual and theoretical value:

$$\eta_{C_F} = \frac{C_{F \exp}}{C_{F \text{theo}}} = \frac{F / (p_c A_t)}{C_{F \text{theo}} \left(\gamma, \frac{A_e}{A_t}, \frac{p_{\text{amb}}}{p_c} \right)}$$

It allows for quantifying the amount of losses within the divergence portion of the nozzle associated to the main sources of performance degradation, such as divergence loss, heat loss, kinetic loss, eventual separation loss, etc.

Since the experimental campaign at sea level has been carried out with a nozzle almost matched with the atmosphere in order to avoid the additional separation losses, its expansion area ratio (2.25) is far from the foreseen one for vacuum (330). Moreover, the nozzle is conical and its typical thrust coefficient efficiency is lower than the one expected for a bell-contoured nozzle due to higher divergence losses. Therefore, the extrapolation of the vacuum specific impulse can include both the corrections due to the different expansion area ratio and the different nozzle shape.

Another important parameter, especially for thrusters intended to be used in the reaction control system, is the response time, conventionally defined as the time necessary for the thrust profile (or eventually the chamber pressure profile) to pass from 1% to 90% of its steady-state value.

Finally, the thrust is considered smooth when the eventual oscillations of the thrust profile are less than 5% of its steady state value.

The typical parameters used for assessing the effectiveness of the combustion of the propellants for thrust generation is the characteristic velocity efficiency (η_{c^*}) defined as:

$$\eta_{c^*} = \frac{c_{exp}^*}{c_{theo}^*} = \frac{\frac{p_c A_t}{m}}{\sqrt{\frac{RT_{ad}}{\gamma} \left(\frac{\gamma+1}{2} \right)^{\frac{\gamma+1}{2(\gamma-1)}}}}$$

The c^* efficiency expresses the ratio between the measured characteristic velocity (obtained from the outputs of the chamber pressure transducer and the flowmeters) and the theoretical one (computed using the 1D ideal rocket equations and the nominal adiabatic combustion temperature, T_{ad} , of the propellants). The c^* efficiency is the key propulsive parameter that takes into account both the degree of the completeness of the combustion, which can reduce the combustion temperature below its nominal value, and the non-idealities of the gas transit through the thrust chamber and the convergent part of the expansion nozzle.

3 EXPERIMENTAL CAMPAIGN ON THE COAXIAL INJECTORS

The final type of injector selected for the steady-state bipropellant thruster is the coaxial injector. Since the propyne presents a quite high value of the vapor pressure at room temperature, the flashing capability of the fuel can be used for a fine atomization of both the propellants in a suitable design coaxial configuration. In order to investigate easily several configurations, the off-the-shelf air atomizing nozzles produced by Spray System Co. (see Figure 5) have been selected for a preliminary screening of the injectors performed with simulant fluids (such as water for hydrogen peroxide and LPG for propyne). The main advantage of these air atomizing nozzles is the possibility of modifying both the inner diameter and the height of the annulus by simply changing whether the air cap or the fluid cap, as shown in Figure 5. The external mix set-up permits to control independently the flows of the propellants and it is mandatory in case of hypergolicity of the propellants. The internal mix set-up produces a finer atomization of the propellants but the propellants streams are no more independent and they affect one another.

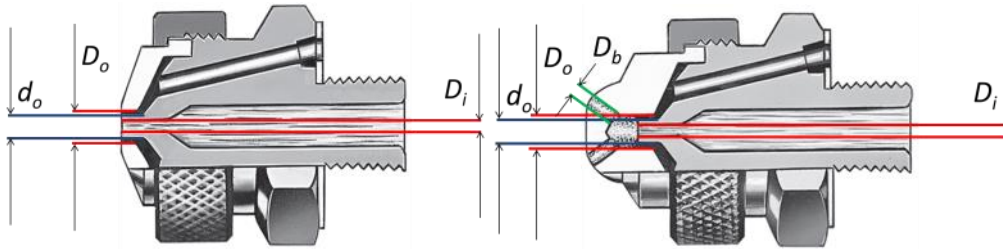


Figure 8. Nomenclature of the external mix set-up (left) and internal mix set-up (right).

Figure 8 (left) reports the nomenclature of the air atomizing nozzles for external mixing. The Fluid Cap is identified with a code, $PF D_i d_o$, that includes information about the diameter of the internal bore and the inner diameter of the annulus, both reported in inch/1000: the code PF1650 means that the diameter of the internal bore of the fluid cap is $D_i=16/1000$ inch and the inner diameter of the annulus is $d_o=50/1000$ inch. The Air Cup code for external mix includes only the outer diameter of the annulus, $PA D_o$; the code PA64 means that the outer diameter of the annulus is $D_o=64/1000$ inch. The nomenclature for the internal mix set-up is shown in Figure 8 (right). The Fluid Cup nomenclature is the same of the previous case while the Air Cup code ($PA D_o N D_b$ -deg) for the internal mixing includes also information about the number (N) and the size (D_b) of the bores in the dome and their cone angle: the code PA67-6-20-70 means that there are six bore with a diameter $D_b=20/1000$ inch with a cone angle of 70° .

Before the experimental campaign on the bipropellant thruster demonstrator with the actual propellants, a preliminary test campaign on the coaxial injectors has been carried out with the aim of assessing the best configuration. This test campaign comprises two phases:

- assessment of the discharge coefficient of the coaxial injectors: for each of the nozzles (whether inner bore or annulus) the discharge coefficient is evaluated using bidistilled water as working fluid;
- assessment of the injection patterns of the coaxial injectors: for each configuration of the coaxial injectors, the atomization and mixing of the propellants are investigated using non-reacting simulant fluids by means of a high-speed camera.

In order to obtain reliable results concerning the injection patterns of the coaxial injectors, the non-reacting simulant fluids should have the physical properties relevant for the injection as close as possible to the actual propellants. To mimick the behavior of hydrogen peroxide, water is typically used as simulant fluid. Except for the slightly higher density of hydrogen peroxide, these two fluids present very close physical properties, as shown in Table 3. A mixture of propane (70%) and butane (30%) has been selected as non-reacting simulant fluid for the propyne. As reported in Table 3, the properties at 15°C of the chosen LPG mixture are very close to the ones of propyne. Moreover, both the propyne and the selected LPG mixture are very sensitive to the operating temperature and,

therefore, an even better overlapping of the properties can be obtained by simulating propyne at 25°C with the propane-butane mixture at 15°C.

Properties @ 15°C	98% H ₂ O ₂	H ₂ O	C ₃ H ₄	C ₃ H ₈ +C ₄ H ₁₀
Density [kg/m ³]	1443	998	627	530
Dynamic Viscosity [Pa s]	0.0014	0.0012	1.52×10 ⁻⁴	1.30×10 ⁻⁴
Vapour Pressure [Pa]	147	1644	432327	561790
Surface Tension [N/m]	0.0737	0.0762	0.0126	0.0095

Table 3. Comparison between the properties of the actual propellants and the non-reacting simulant fluids.

The tests with simulant fluids have been carried out in the same test rig of the bipropellant thruster demonstrator. The architecture of the facility allows for controlling the mass flow rates of the propellants by means of two cavitating venturis located along the oxidizer and fuel lines. As long as the cavitating venturis are in cavitating regime, the mass flow rates are controlled only by the pressures inside the tanks of the propellants. In order to understand how close are the experiments with the simulant fluids to the actual configuration with the real propellants, some preliminary computations have been performed with the following assumptions:

- same geometry: the geometry of the coaxial injector is fixed as reported in Table 4 for both the simulant fluids and the actual propellants;
- same mass flow rate control devices: the same cavitating Venturis are used to control the mass flow rates of the simulant fluids and the actual propellants.

The nominal tank pressure in both the tanks for the bipropellant thruster demonstrator is 35 bar. The range of the tank pressure investigated in the simulations is from 25 bar to 40 bar.

As reported in Figure 9, the mass flow rates of the simulant fluids are lower with respect to the actual propellants. In particular, the mass flow rate of water is much more reduced and, therefore, also the mixture ratio of the simulant fluids is lower with respect to the actual case.

Injector	D_i	d_i	D_o	A	C_d
	[mm]	[mm]	[mm]	[m ²]	[--]
PF1650	0.406	N/A	N/A	1.30×10 ⁻⁷	0.87
PA64	N/A	1.27	1.63	8.09×10 ⁻⁷	0.66

Table 4. Coaxial injector configuration selected for the preliminary assessment of the effect of the simulant fluids.

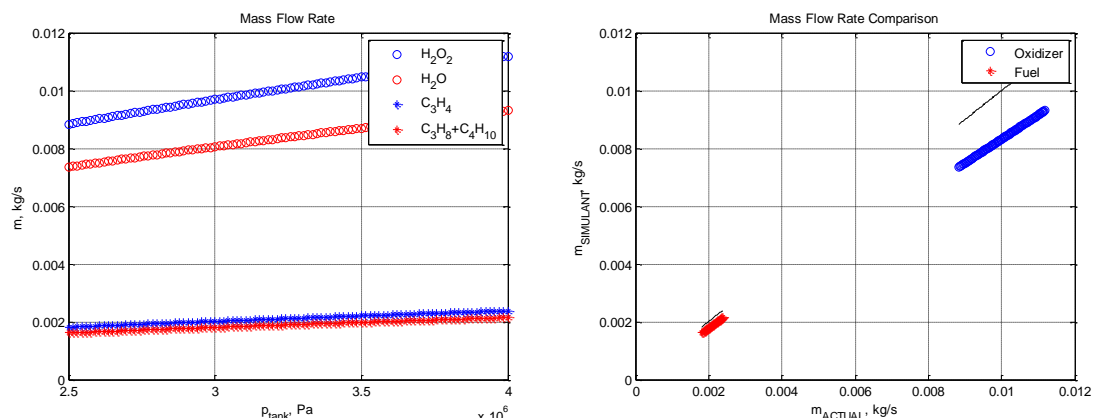


Figure 9. Comparison between the mass flow rates of the simulants and the actual propellants.

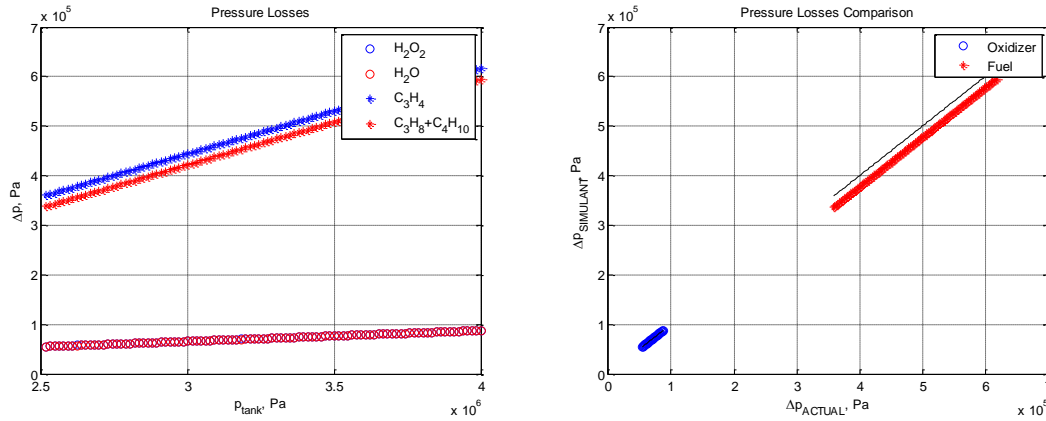


Figure 10. Comparison between the pressure losses across the injectors with the simulants and the actual propellants.

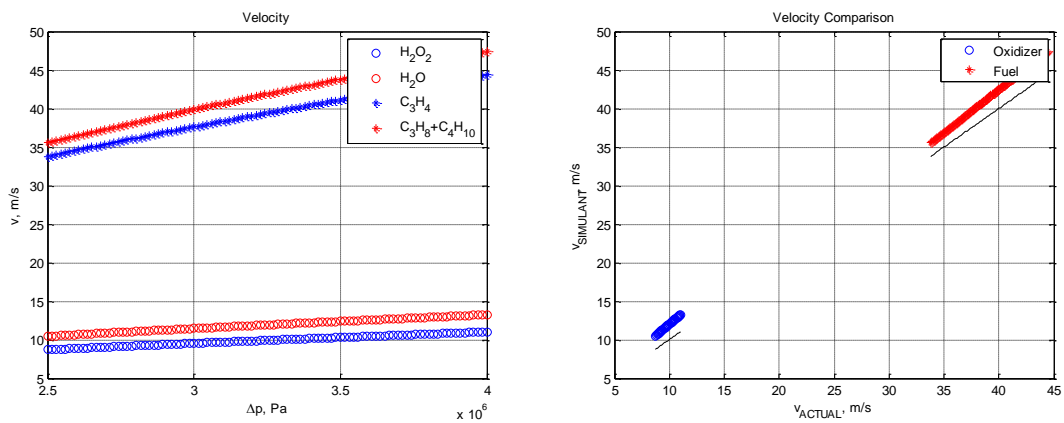


Figure 11. Comparison between the velocities across the injectors with the simulants and the actual propellants.

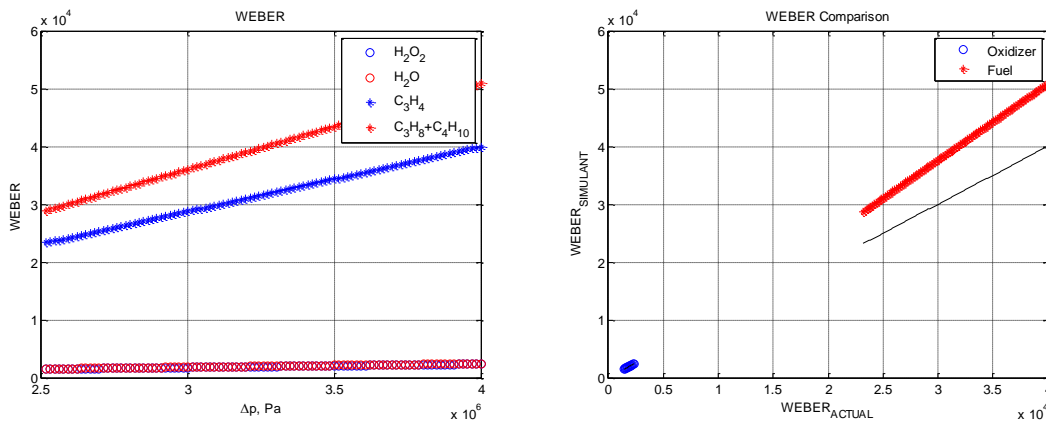


Figure 12. Comparison between the Weber numbers of the injectors with the simulants and the actual propellants.

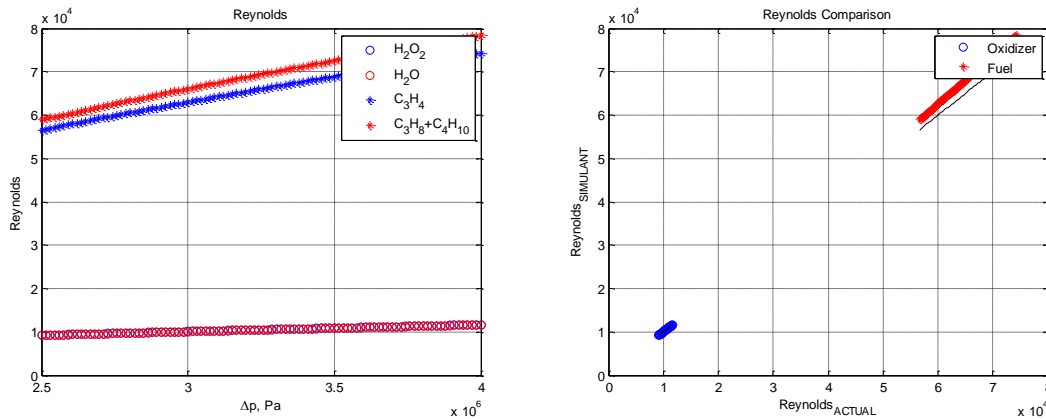


Figure 13. Comparison between the Reynolds numbers of the injectors with the simulants and the actual propellants.

However, the values of the mixture ratio (4.7 for the actual propellants, 4.3 for the simulant fluids) are still very close and the results of the simulant fluids can be still considered relevant for mimicking the actual injection patterns.

The other relevant parameters for the injection patterns are:

- pressure drop across the injectors:

$$\Delta p = \frac{1}{2\rho} \left(\frac{m}{C_d A_i} \right)^2$$

as shown in Figure 10, for the oxidizer the pressure drop across the injector are almost the same for hydrogen peroxide and water (the vapour pressure of both the fluids is negligible with respect to the nominal tank pressure). Even if the pressure losses in the injector of the fuel differ for LPG and propyne (the vapor pressure of both the fluids is not negligible with respect to the nominal tank pressure and is slightly different for the considered fluid), they are very close and the similarity condition is fulfilled;

- injection velocity:

$$v_i = \sqrt{2 \frac{\Delta p}{\rho}}$$

because of the lower density, the injection velocities for the simulant fluids are higher than the ones of the actual propellants. Even in this case, the discrepancy is low and acceptable (see Figure 11);

- Weber number:

$$We = \left(\frac{\rho v_i^2 d}{\sigma} \right)$$

this adimensional number is really critical for the determination of the injection patterns. For the oxidizer, there is an almost perfect overlapping of the curves for the simulant fluids and the actual propellants. Moreover, the small gap for the fuel case is totally acceptable because both the curves have the same order of magnitude and the difference for a fixed tank pressure is really small (see Figure 12);

- Reynolds number:

$$Re = \left(\frac{\rho v_i d}{\mu} \right)$$

Also the Reynolds number that takes into account the viscous forces confirms that the similarity criterion is fulfilled (see Figure 13).

The results of this preliminary analysis are really promising since almost all the critical parameters confirm the effectiveness of the similarity approach with the selected non-reacting simulant fluids, especially in terms of atomization and mixing capability of the fluids.

3.1 Assessment of the Discharge Coefficient with Water

The discharge coefficient of an injector of know geometry (such as the area of the injector A_i)

$$C_d = \frac{m}{A_i \sqrt{2\rho\Delta p}}$$

can be simply obtained by measuring the mass flow rate passing through the injector (m) for a fixed pressure drop across the device (Δp), once the properties of the working fluid are known (such as the density ρ).

Injector	D_i [mm]	d_i [mm]	D_o [mm]	A [m ²]	Δp [bar]	$m_{\text{flowmeter}}$ [g/s]	m_{scale} [g/s]	$C_{d(\text{flowmeter})}$ [--]	$C_{d(\text{scale})}$ [--]
PF16100	0.406	N/A	N/A	1.30×10^{-7}	10.28	5.10	5.17	0.86	0.87
					8.80	4.72	4.80	0.87	0.89
					7.79	4.37	4.60	0.85	0.89
					6.95	3.91	4.36	0.81	0.90
					5.48	3.65	3.90	0.85	0.90
					4.90	3.50	3.59	0.86	0.88
					4.16	3.23	3.38	0.86	0.90
					3.29	2.90	3.10	0.87	0.93
PF28100	0.711	N/A	N/A	3.97×10^{-7}	1.46	6.44	6.60	0.95	0.97
					2.29	8.01	8.44	0.94	0.99
					3.05	9.48	9.76	0.96	0.99
					3.85	10.64	10.97	0.96	0.99
					4.58	11.70	12.19	0.97	1.00
PA64	N/A	1.27	1.63	8.09×10^{-7}	1.35	8.80	8.65	0.66	0.65
					1.94	10.60	10.53	0.66	0.66
					2.88	12.60	12.74	0.65	0.65
					3.86	14.80	14.73	0.66	0.65
					4.67	16.06	16.04	0.65	0.65
PA104	N/A	2.54	2.64	4.13×10^{-7}	1.58	3.48	3.67	0.47	0.49
					2.42	4.60	4.95	0.50	0.543
					3.27	5.30	5.58	0.50	0.52
					4.38	6.40	6.76	0.52	0.55
					5.30	7.10	7.42	0.53	0.55
PA108	N/A	2.54	2.80	1.09×10^{-6}	1.16	11.45	12.10	0.68	0.73
					1.84	14.77	15.93	0.70	0.76
					2.68	18.68	19.25	0.74	0.76
PA120	N/A	2.54	3.05	2.23×10^{-6}	4.26	13.10	13.02	0.64	0.63
					10.86	23.20	20.54	0.70	0.62

Table 5. Discharge coefficient for the air atomizing nozzle produced by Spray System Co.

Table 5 reports the results of the test campaign with bidistilled water performed for the evaluation of the discharge coefficient of the candidate Fluid Caps and Air Caps. The mass flow rate has been measured by means of two different approaches: using a Coriolis flowmeter; and collecting the water in a vessel and, then, measuring its weight by means of a scale and the overall time of the experiment with a chronometer.

In general, the internal bore of the Fluid Cap shows a quite high value of the discharge coefficient that can range from 0.85 to 0.99. On the contrary, the discharge coefficient of the annulus is lower and its typical value is between 0.5 and 0.7. The discharge coefficients of the Fluid Caps PF1650 and PF2850 have not been experimentally assessed, since they are supposed to be equal to PF16100 and PF28100, respectively. Finally, the evaluation of the discharge coefficients of the Air Caps PA67-6-20-70 and PA120-6-35-60 is not trivial since the inner and outer streams are not independent. It has been decided to test them directly with the simulant fluids.

3.2 Injection Patterns with Simulant Fluids

As a result of the experimental assessment of the discharge coefficient of the nozzles, eight different configurations of the coaxial injectors have been identified for the next experimental campaign on the flow patterns with simulant fluids, as reported in Table 6.

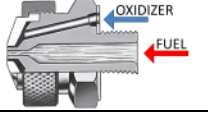
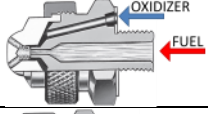
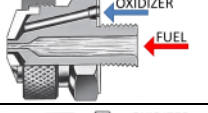

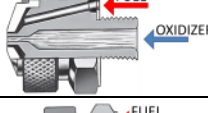
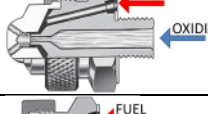
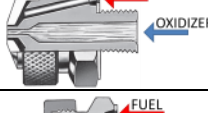

Fluid Cap	Air Cap	Inner/Outer	Mix Set-Up	Layout
PF1650	PA64	Fuel/Oxidizer	External	
PF1650	PA67-6-20-70	Fuel/Oxidizer	Internal	
PF16100	PA108	Fuel/Oxidizer	External	
PF16100	PA120-6-35-60	Fuel/Oxidizer	Internal	
PF28100	PA104	Oxidizer/Fuel	External	
PF28100	PA120-6-35-60	Oxidizer/Fuel	Internal	
PF2850	PA64	Oxidizer/Fuel	External	
PF2850	PA67-6-20-70	Oxidizer/Fuel	Internal	

Table 6. Coaxial injector configurations tested with the simulant fluids.

The main aim of these tests is to study, at least qualitatively, the interaction between the fuel and oxidizer streams, especially in terms of effectiveness of the atomization and mixing processes.

Coaxial injector: fuel inner/oxidizer outer

Due to its high vapor pressure, the fuel (and, consequently, its simulant fluid) flashes when it is injected in an ambient at atmospheric pressure. As a result, the jet of fuel through the inner bore

tends to expand in the radial direction, thus enhancing the mixing of the two streams and, consequently, the atomization of the fluids.

For each of the coaxial injector configurations, the typical test sequence comprises three injections:

- a ten seconds injection of only the fuel (i.e. its simulant fluid);
- a ten seconds injection of only the oxidizer (i.e. its simulant fluid);
- a ten seconds injection of the fuel and the oxidizer together.

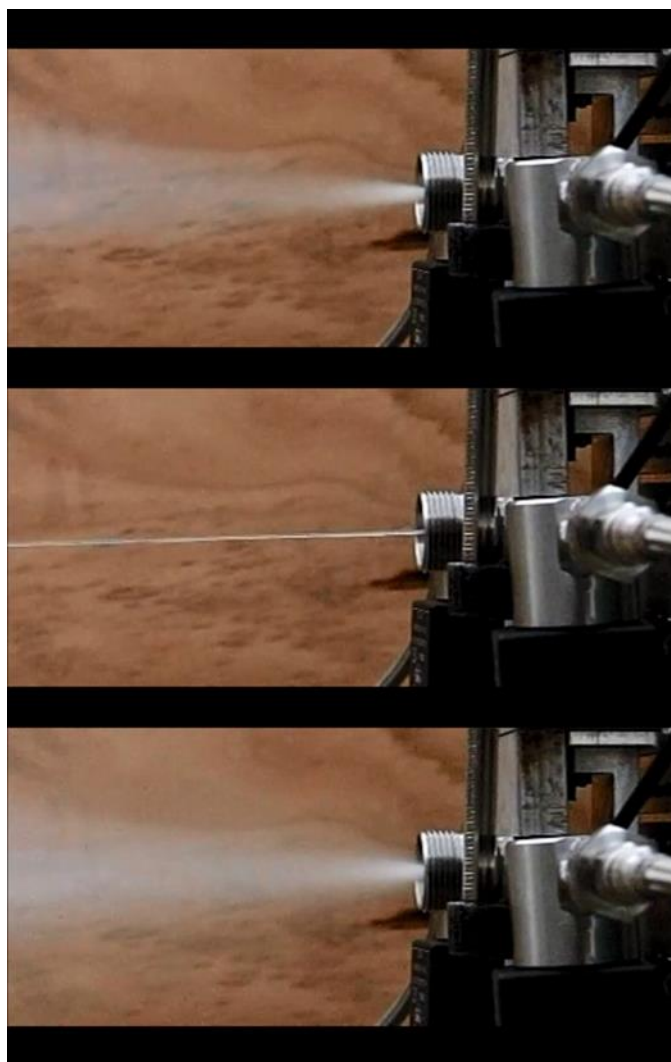


Figure 14. Jet patterns for PF1650+PA64: butane-propane mixture through the inner bore (top); water through the annulus (middle); water and butane-propane mixture together through the coaxial injector (bottom).

The first configuration analyzed was the external mix set-up obtained with PF1650+PA64. Along the oxidizer line, the tank pressure was set to the nominal value (35 bar) and the mass flow rate measured by the Coriolis flowmeter reached the desired value because the cavitating Venturi worked correctly. As expected, the pressure drop across the injector was between 1 bar and 1.5 bar.

The pressure inside the tank of the fuel was fixed to the nominal value. Both the inlet and outlet pressure of the Venturi confirm that the device correctly worked in cavitating regime. The pressure losses across the fuel injector were significantly higher than the expected ones (13 bar instead of 6 bar) but still compatible with the nominal operating condition of the bipropellant thruster demonstrator. The more likely reason of this behaviour is the flashing of the fuel at the exit of the

nozzle. Concerning the O/F ratio, the outputs of the cavitating Venturi assure that the tests were performed almost at the nominal condition and, therefore, they can be considered relevant for the characterization of the injection patterns. Figure 14 reports pictures of the three injections. The simulant of the fuel injected through the inner bore creates a jet that is expanding because the fluid starts flashing. On the contrary, the water injected through the annulus produces a jet with a quite long compact length in which the liquid tends to close the gap of the annulus and form a compact full jet. The combination of the two streams is really effective since there are a very good mixing and a fine atomization of the two non-reacting simulant fluids. Qualitatively, the flow patterns of this configuration proved to be really effective.

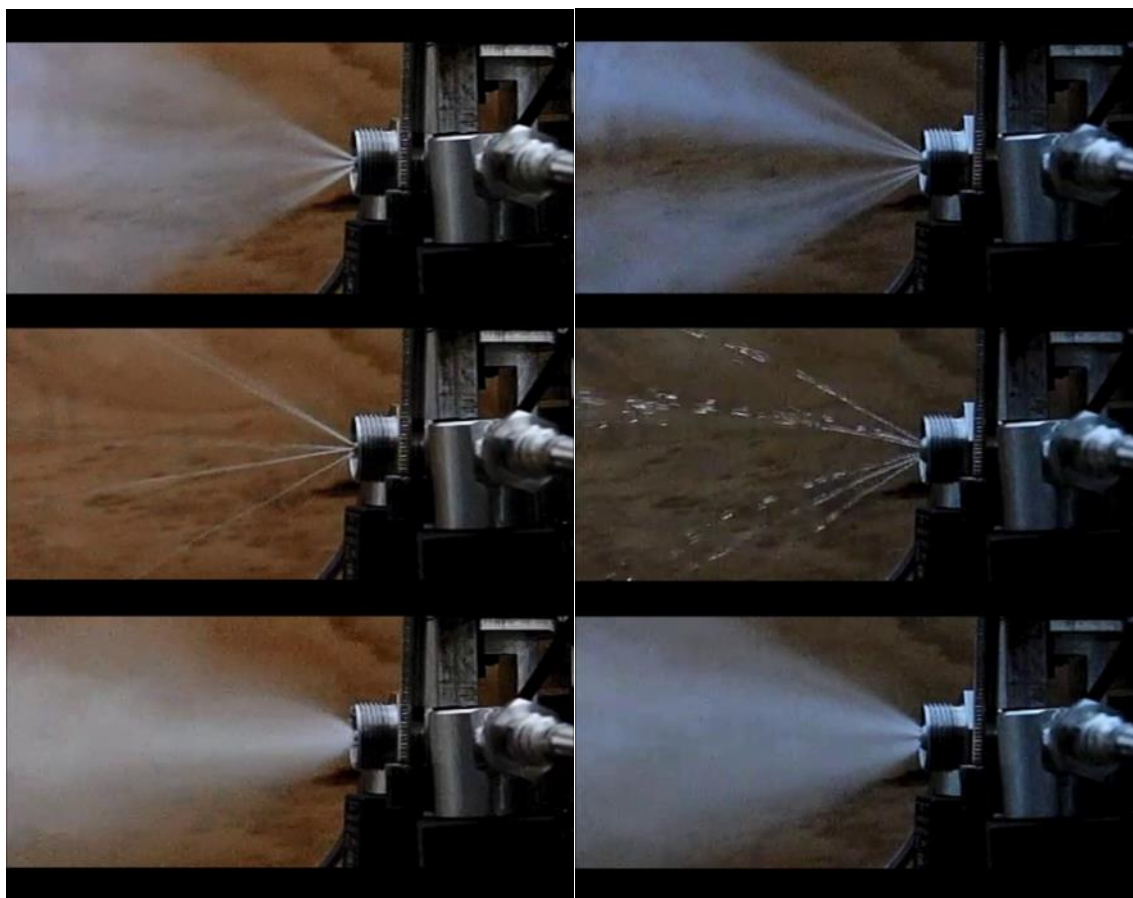


Figure 15. Jet patterns for PF1650+PA67-6-20-70(left) and PF16100+PA120-6-35-60(right): butane-propane mixture through the inner bore (top); water through the annulus (middle); water and butane-propane mixture together through the coaxial injector (bottom).

In the internal mix set-up configuration PF1650+PA67-6-20-70, the two streams are not independent. However, since the mass flow rates were effectively controlled by the two cavitating Venturis, the interaction between the two streams is only in terms of change of the pressure losses and not in terms of mass flow rate or O/F ratio. The experimental data confirmed that the Venturis correctly worked and, consequently, the O/F ratio obtained during the third injection with both the fluids was very close to the nominal condition. The pictures that highlight the injection patterns of the three tests are reported in Figure 15 (left). Concerning the injection of only the simulant of the fuel, the jet is now divided in six streams because of the six bores on the dome of the Air Cap. The flashing behaviour of the fluid is still evident in the progressive vaporization of six jets initially injected in liquid phase. The test with only water shows that the six jets exiting from the bores present a quite long compact jet with high velocity. The combination of the two streams proved to be really effective for

the atomization and mixing of the propellants, especially because the internal mixing configuration allows first to finely mix the fluids inside the injector and then to obtain an atomized spray through the bores of the dome of the Air Cap (see the picture on the bottom of Figure 15 - left). Moreover, with respect to the previous configuration (PF1650+PA64), the internal mix set-up produces a final atomized spray that is more spread in radial direction and, therefore, it allows for obtaining the necessary high atomization of the propellants within a shorter distance from the outlet of the nozzle. The next configuration tested has been the PF16100+PA108 injector. This configuration is very similar to the PF1650+PA64 because the inner bore of the Fluid Cup is the same. Only the height of the annulus and the distance between the annulus and the inner bore are different. The injection patterns for the PF16100+PA108 configuration are very similar to the ones obtained with the PF1650+PA64 configuration. However, the higher gap between the stream of the inner bore and stream through the annulus implies a less effective atomization of the final spray. In conclusion, due to the slightly worse injection patterns the PF16100+PA108 configuration is less attractive than the PF1650+PA64 configuration.

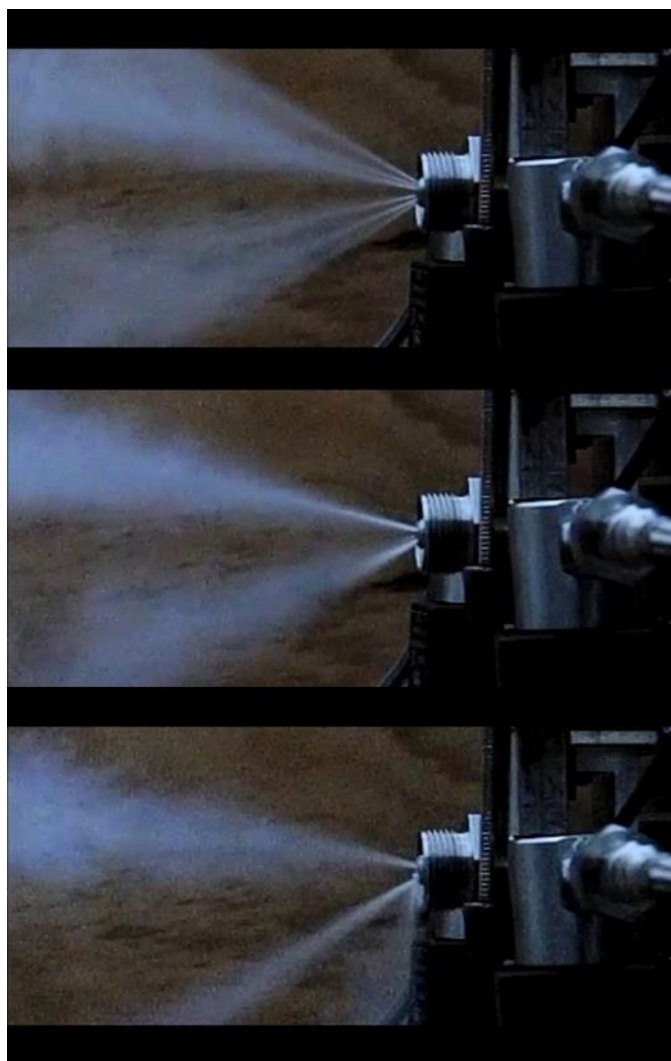


Figure 16. Jet patterns for butane-propane mixture through the inner bore of the PF16100+PA120-6-35-60 configuration: beginning of the test (top); middle of the test (middle); end of the test (bottom).

The last configuration tested with the fuel passing through the inner bore of the coaxial injector was the PF16100+PA120-6-35-60 internal mix set-up. With respect to the PF1650+PA67-6-20-70, both

the area of the annulus and the overall area of the bores on the dome of the injector are higher. Even if in this configuration the spray is a finely atomized (see Figure 15, right-bottom), the resulting spray presents a wider cone angle of the jet with respect to the PF1650+PA67-6-20-70, probably because of the reduced velocity of the water. In view of the final utilization inside the bipropellant thruster demonstrator, the previous configuration seems to be better.

Moreover, during the test with only the simulant fluid of the fuel, the reduced velocity across the six bores of the dome allowed for occluding some of the bores because of the freezing of the flashing fluid, as shown in Figure 16. This problem did not occur during the test with both the fluids (see Figure 15 - right). However, this fact together with the wider angle of the atomized spray with respect to the previous internal mix set-up configuration suggests that the best candidate for the internal mix set-up with the fuel passing through the inner bore is the PF1650+PA67-6-20-70 configuration.

Coaxial injector: oxidizer inner/fuel outer

In the external mix set-up, when the oxidizer or its simulant fluid passes through the inner bore, the atomization and the mixing of the propellants are enhanced by the different velocities between the two fluids in the shear layer between the inner jet and the outer annulus. In this case, the flashing of the fuel implies a dramatic increase of the velocity of the stream in the annulus since the density varies a lot from the liquid to the vapor phase.

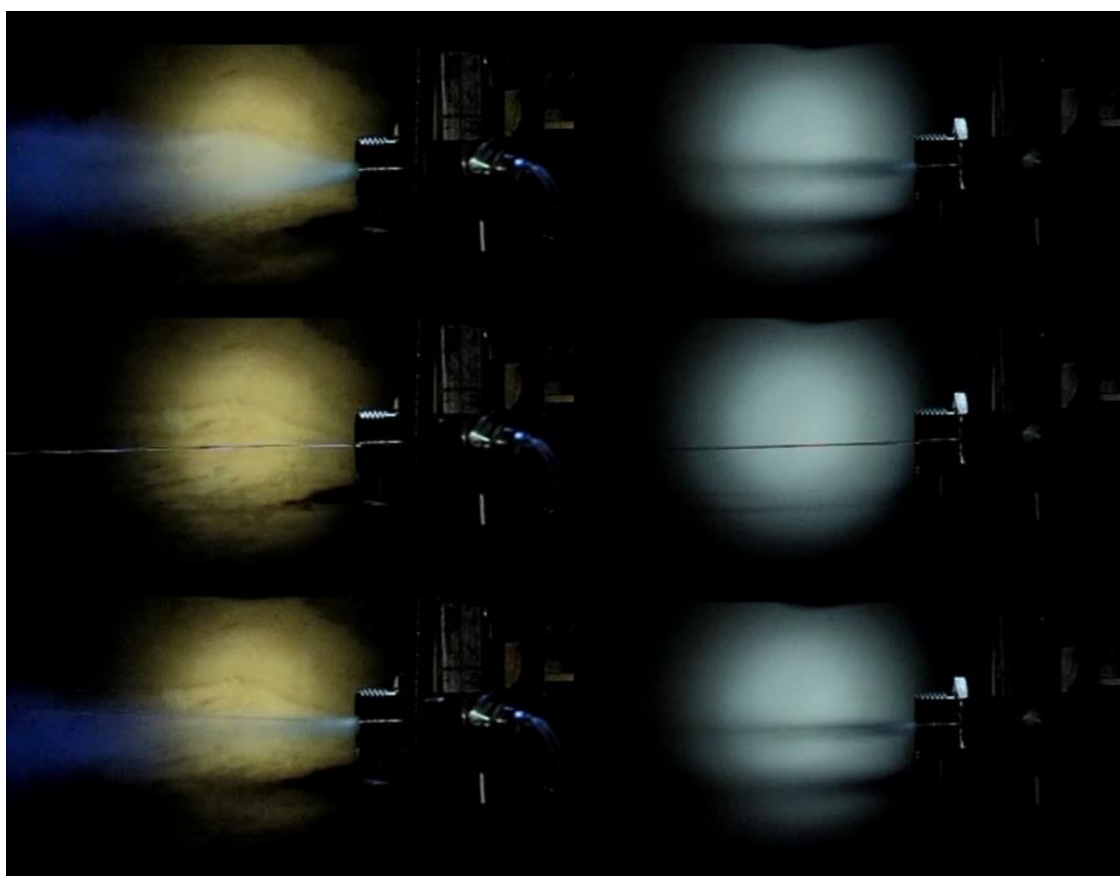


Figure 17. Jet patterns for PF28100+PA104 (left) and PF2850+PA64 (right): butane-propane mixture through the inner bore (top); water through the annulus (middle); water and butane-propane mixture together through the coaxial injector (bottom).

The first configuration tested has been the PF28100+PA104. This configuration is an external mix set-up in which the two streams are independent. Due to the lower discharge coefficient of the annulus of the outer stream, the pressure losses of the oxidizer increased while the pressure drop of the fuel decreased with respect to the previous configuration with switched streams (fuel inner/oxidizer outer). The nominal flow rate was almost perfectly guaranteed in both the oxidizer and fuel line, together with the nominal O/F ratio. Concerning the jet patterns reported in Figure 17 (left), the results were not promising. The injection of the fuel in the outer annulus produced a highly vaporized jet due to the flashing of the simulant fluid of the fuel. On the contrary, the jet of water through the inner bore is fast and compact with a very long compact length. As reported in the bottom picture of Figure 17 (left), the interaction between the two streams was weak since the inner water jet continued to be compact inside the flashed conical jet of the outer stream of LPG. The reason of the low interaction may rely also the quite high gap between the inner bore (28/1000 inch) and the inner diameter of the annulus (100/1000 inch). This configuration was definitively not effective in terms of the mixing and atomization of the two streams and, therefore, it is not recommended for the use in the bipropellant thruster demonstrator.

The last external mix set-up tested is the PF2850+PA64 configuration. In this coaxial injector, the inner bore and the annulus are closer with respect to the PF28100+PA104 assembly. The jet patterns of the three injections are reported in Figure 17 (right). Even if in this configuration the inner bore and the annulus were closer, the atomization and mixing resulting from the simultaneous injection of both the fluids were poor. In fact, the compact jet of water is still visible inside the annular jet of the simulant fluids of the fuel. As for the PF28100+PA104, the external mix set-up with the low-vapour pressure fluid (oxidizer or its simulant) located in the inner bore proved to be not suitable for obtaining a finely atomized spray. Therefore, this configuration is not recommended for the final design of the bipropellant thruster.

The results of the internal mix set-up for the PF28100+PA120-6-35-60 are shown in Figure 18 (left). The Air Cap has been already tested in the previous experimental campaign, however in this configuration the streams of the propellants are switched from the inner to the outer and vice versa. Despite the wider inner bore of Fluid Cap PF28100, the pressure drop for the water at the nominal flow rate were quite high, such as 3 bar. On the contrary, the quite large gap of the annulus for the simulant of the fuel yielded to an inlet injector pressure lower than the vapor pressure of the working fluid. This implies that the cavitating Venturi was in breakdown condition and the flow after the Venturi was likely a two-phase flow. At breakdown, the exit flow can be highly unstable and, even if the estimation of the mass flow rate by means of the Cavitating Venturi is still reliable, it is better to be far from this condition in order to avoid the onset of flow instabilities in the combustion chamber. In terms of spray patterns, the injection of only the fuel showed a rapid flashing of the propellants that was injected already in two-phase flow, as shown in Figure 18 (left). The six compact jets of water (see middle of Figure 18 - left) were highly atomized when the coaxial injector was operated with both the fluids (see bottom of Figure 18 - left). Even in this case, the spray cone angle was quite high, thus resulting in an undesired impinging of the propellants on the internal walls of the combustion chamber. In conclusion, the experimental campaign on the PF28100+PA120-6-35-60 coaxial injector confirms that this configuration is not suitable for the use in the bipropellant thruster demonstrator mainly because the pressure losses across the injector do not allow for avoiding the breakdown condition of the cavitating Venturi during the initial start-up transient.

Finally, the internal mix set-up PF2850+PA67-6-20-70 was also tested with the simulant fluids. The nominal value of the mass flow rate of the fuel produced a pressure drop equal to 3 bar. On the contrary, the pressure losses across the fuel injector, equal to 4 bar, allowed for maintaining liquid the LPG between the outlet of the Venturi and the injector). During the test with both the fluids, the interaction between the fluids, typical of the internal mix set-up, produced an increase of the pressure losses across the injector in both the lines. Figure 18 (right) shows the pictures of the three consecutive injections. The fuel showed the typical flashing behaviour already highlighted in the previous experiments. The water jets across the six bores of the dome of the injector had a very short compact length, since the jets started to break into droplets a few centimeter from the outlet of

the nozzle. The final combined jet with both the fluids proved to be very effective in atomizing and mixing both the fluids. In terms of injection patterns, the atomized spray is very close to the case of the PF1650+PA67-6-20-70 (see Figure 14). The main difference is the lower pressure drops across the injector, especially through the fuel line.

In conclusion, the best injector configurations selected for the next tests with the bipropellant thruster demonstrator are:

- external mix set-up PF1650+PA64 (inner fuel/outer oxidizer);
- internal mix set-up PF1650+PA67-6-20-70 (inner fuel/outer oxidizer);
- internal mix set-up PF2850+PA67-6-20-70 (inner oxidizer/outer fuel).

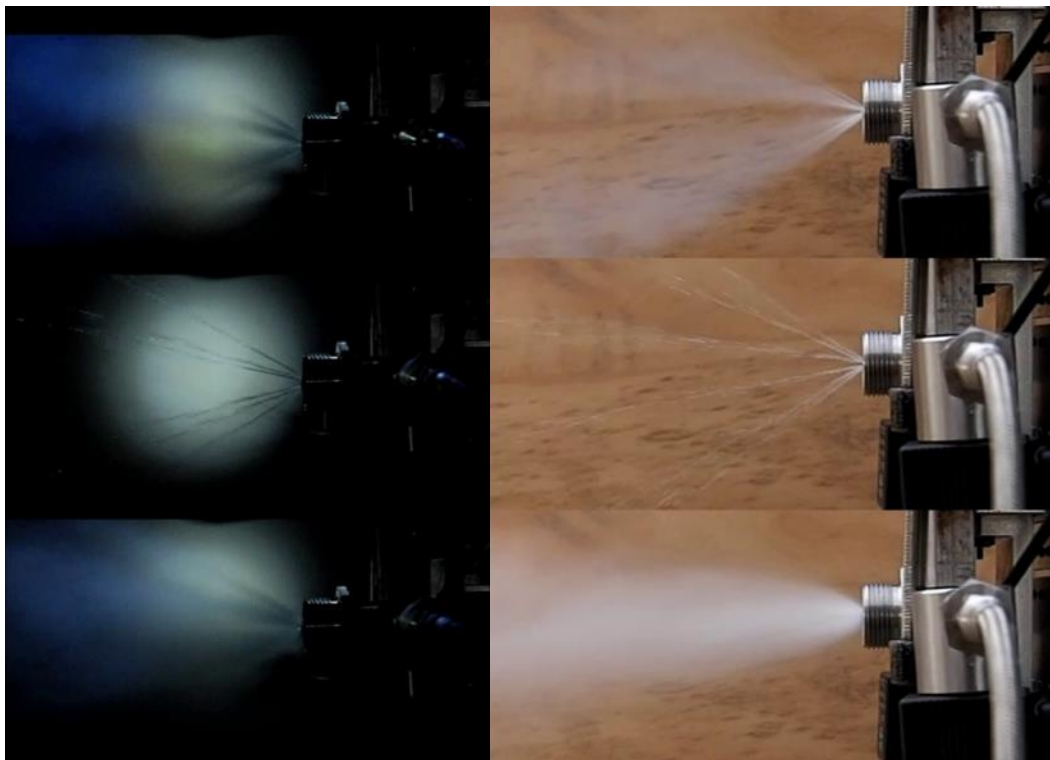


Figure 18. Jet patterns for PF28100+PA120-6-35-60 (left) and PF2850+PA67-6-20-70 (right): butane-propane mixture through the inner bore (top); water through the annulus (middle); water and butane-propane mixture together through the coaxial injector (bottom).

4 EXPERIMENTAL CAMPAIGN ON THE IGNITABILITY OF THE PROPELLANTS

After the tests on the injection system that mainly deals with atomization and mixing efficiencies, the next step is the assessment of the ignitability of the propellants (i.e. the capability of starting the combustion reaction). The following approaches have been experimentally investigated:

- Hypergolicity of the propellants: in this case the propellants start to react when they come in contact.
- Spark Plug as Igniter: the energy releases by the spark plug allows for starting the combustion reaction. Moreover, the spark plug can be used to start the decomposition of propyne, as reported in [24].

All the ignitability tests have been performed at ambient pressure using only the injection manifold without the thrust chamber. The two tested injectors are shown in Figure 19.



Figure 19. The two tested injectors: PF1650+PA64 (left) and PF1650+PA67-6-20-70 (right).

4.1 Hypergolicity Tests

Some tests have been performed in order to understand if the two fluids can directly react without using any source of ignition. Figure 20 shows the injection of propyne only (top), HTP only (middle) and, finally, their contemporary injection (bottom) in order to show if the propellants are hypergolic. The injector used in the tests reported in the following pictures is the PF1650+PA64 that is an external mix set-up more suitable in case of hypergolicity of the propellants. As visible from the different pictures the propyne, centrally injected, tends to flash and produces a vapor coming out of the manifold. The HTP, injected coaxially to propyne, tends to remain liquid and shows a straight liquid jet out of the manifold.

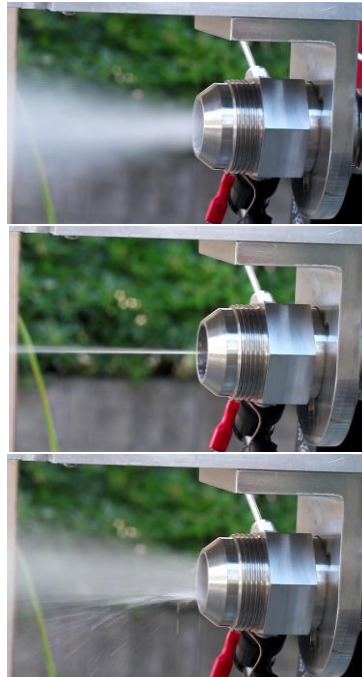


Figure 20. Injection of only propyne (top), injection of only HTP (middle) and contemporary injection of propyne and HTP (bottom) through the injector PF1650+PA64.

As visible from Figure 20 the two propellants, injected at the same time, appear to be partially mixed with some hydrogen peroxide drops coming out of the manifold. However the two propellants did not react: they are not hypergolic. Therefore, some energy must be supplied in order to allow the reaction between the two propellants. As shown in Figure 21, both the cavitating Venturis have been able to guarantee the correct mass flow rate and consequently the nominal O/F ratio.

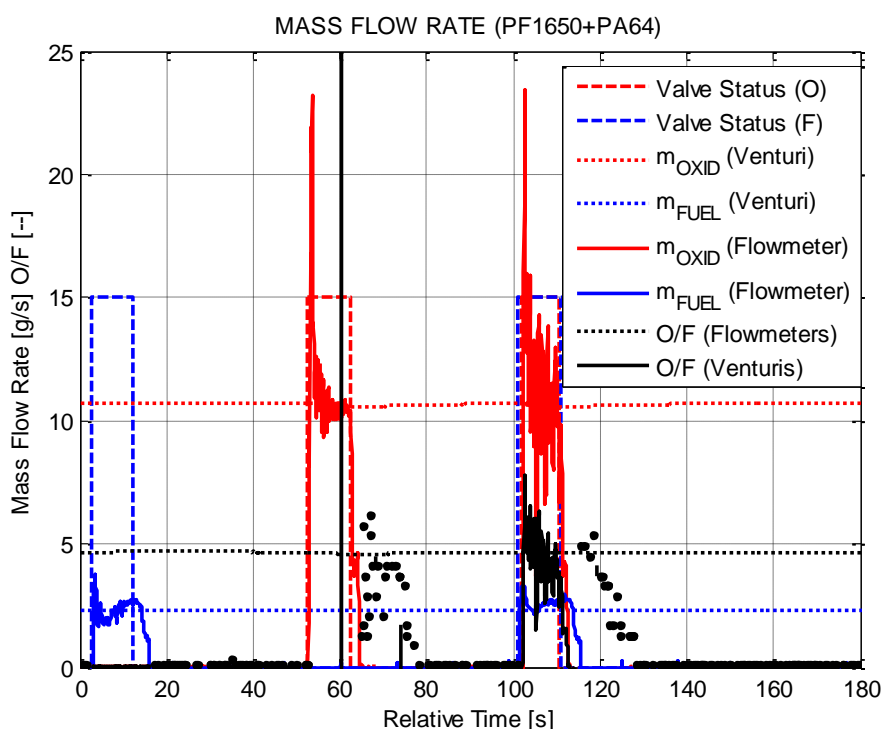


Figure 21. Hypergolicity test with PF1650+PA64: propellants mass flow rates and O/F ratio.

4.2 Spark Plug as Igniter

Some tests have been performed with different injectors in order to assess the capability of a spark plug to ignite the propellants when they are already atomized and mixed. The ignition of the mixture of the propellants has never taken place. It has been decided to cause the decomposition of one of the propellants. In particular, the tests showed that the spark plug is able to cause the decomposition of propyne but not the one of hydrogen peroxide. Therefore, it has been decided to try to use the heat released by propyne decomposition to decompose HTP and thus letting it react with propyne decomposition by-products and fresh injected propyne.



Figure 22. Setup for the tests performed on PF1650+PA64 injector (left) and PF1650+PA67-6-20-70 (right) by using the spark plug.

External mix set-up: PF1650+PA64

Some tests have been performed with this injector and they showed the great easiness to spark the propyne and cause its decomposition with a spectacular flame. The test setup for these tests is shown in Figure 22 (left). Figure 23 shows the sequence of some moments during the experiments.

The figure clearly shows the ignition of the propyne and the consequent flame. The injection of HTP (injected coaxially and externally to the propyne jet) causes the flame shape to be more cylindrical. From the pictures it can be noted that the HTP decomposition is not completed and some hydrogen peroxide still remains in liquid phase out of the manifold.

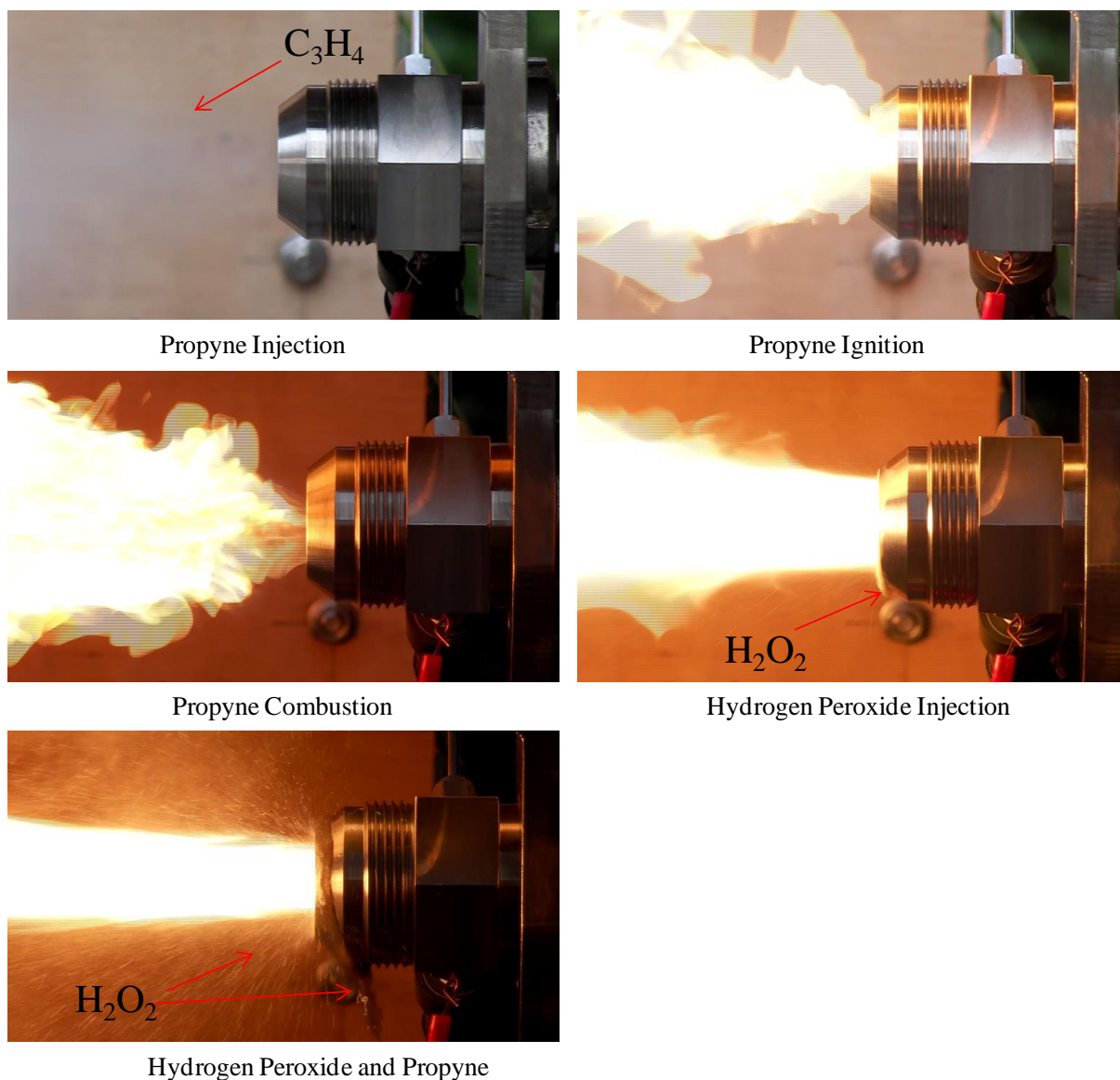


Figure 23. Sequence of different moments during the ignition tests performed with the injector PF1650+PA64 (injection sequence: first propyne, its ignition and then HTP injection and combustion).

The typical ignition sequence comprises the following phase: a first firing pulse with propyne that saturates the injection manifold; when the velocity of propyne decreases the propyne starts to decompose; after the ignition of propyne the firing valve of the fuel is opened again to create an ignited jet of propyne; the final step is the opening of the oxidizer valve that yields to the combustion of both the propellants. As shown in Figure 24, the nominal value of the O/F ratio was obtained even if the output of the oxidizer flowmeter showed strong oscillations around the mean value. The unstable behavior of the oxidizer mass flow rate is mainly due to the highly turbulent combustion and the low pressure drop across the injector.

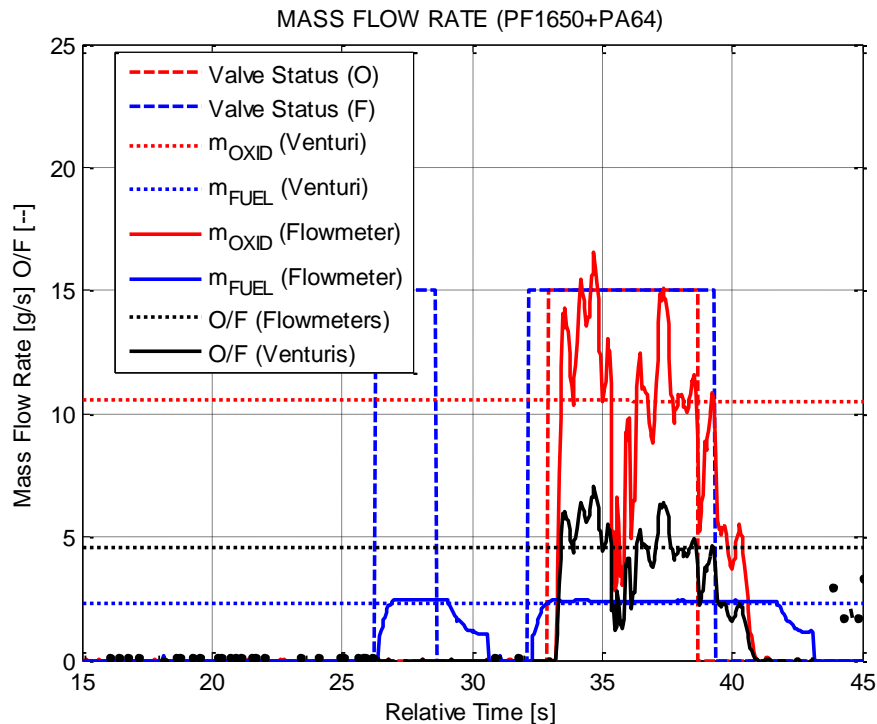


Figure 24. Spark plug as igniter test with PF1650+PA64: propellants mass flow rates and O/F ratio.

In order to appreciate the length of the flame two pictures at greater distance are shown in Figure 25.

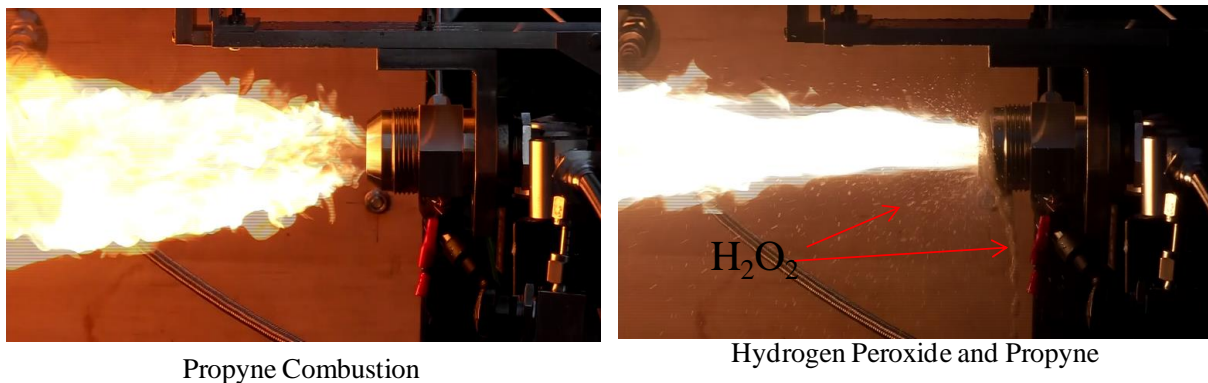


Figure 25. Flames due to propyne decomposition (left) and to hydrogen and propyne combustion (right).

Internal mix set-up: PF1650+PA67-6-20-70

The setup used for the tests performed with this injector is shown in Figure 22 (right). As done with the previous injector, the propyne has been injected first and a spark has been used to start its decomposition and then, if propyne decomposition started, HTP has been injected in order to let the two substances react. The tests performed on this injector showed more difficulties for the ignition of propyne. This is probably due to the particular shape of the injector with six holes which allow for the impingement of the flashing injected propyne with the cold metal manifold. This slows down the evaporating process of propyne which partly drips out of the manifold. When the propyne ignition

happens, the liquid propyne spilled out produces a huge flame which hides the manifold before the HTP is injected. Some pictures of the tests performed are shown in Figure 26.

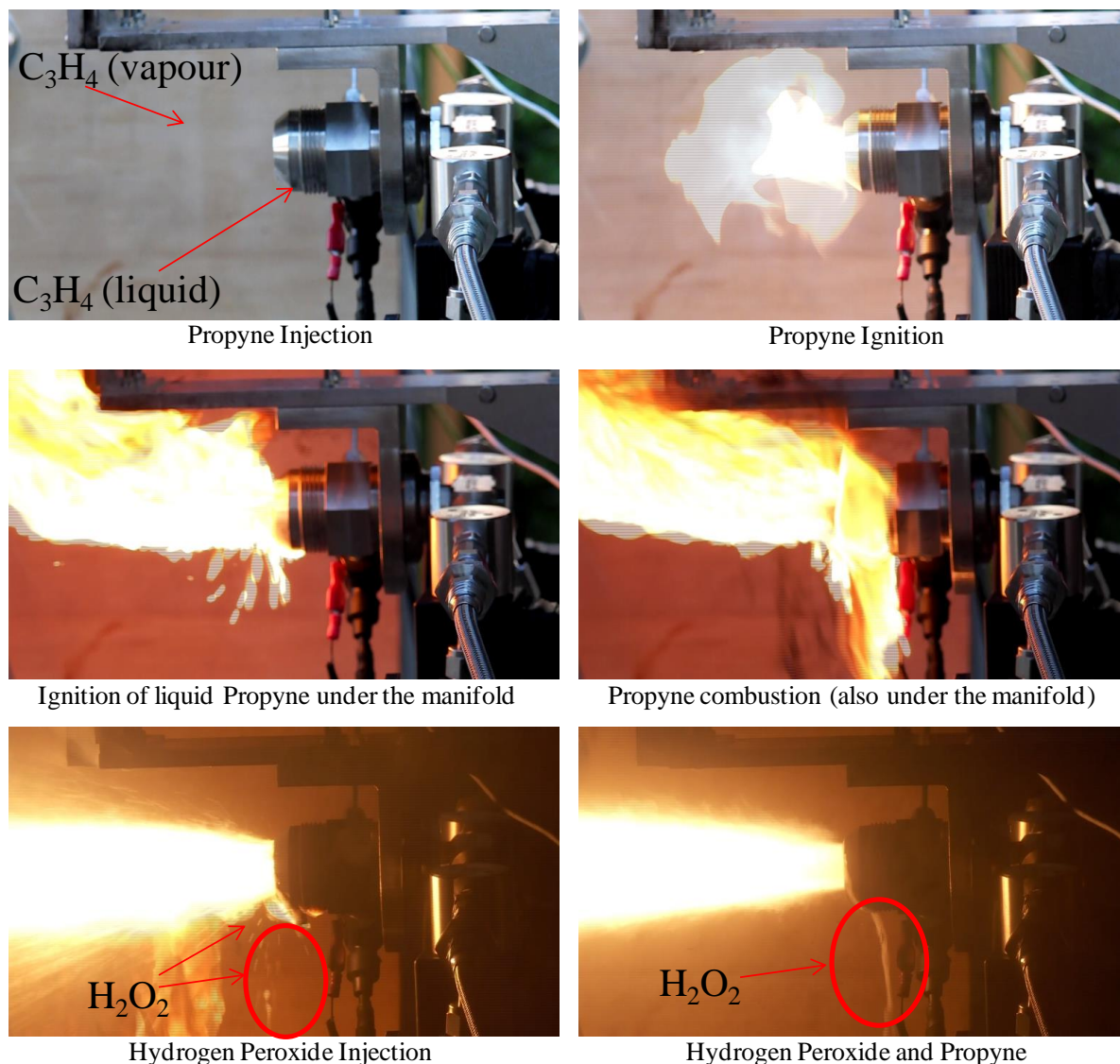


Figure 26. Sequence of events during the ignition tests performed with the injector PF1650+PA67-6-20-70 (injection sequence: first propyne and its ignition and then HTP).

As in the previous case, part of the injected HTP, even passing through a high temperature region, is not able to totally decompose and react with propyne. The HTP dripping out from the manifold is clearly visible. Only after three pulses the propyne has ignited. In this case, due to the higher pressure losses across the oxidizer injector the mass flowrate measured by the Coriolis flowmeter has been smoother and the O/F has been constant at the nominal value. The resulting flame has been particularly strong and uniform.

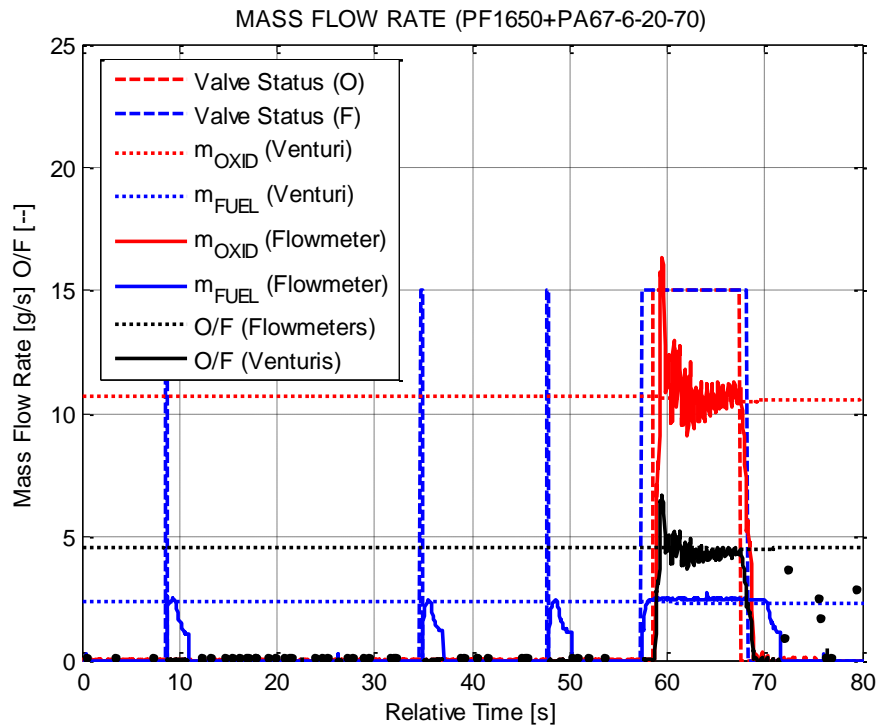


Figure 27. Spark plug as igniter test with PF1650+PA67-6-20-70: propellants mass flow rates and O/F ratio.

An attempt to ignite propyne and HTP, injected at the same time, has been also performed. This attempt has been suggested by the clogging of the six injector holes because of the flashing of propyne and its consequent freezing through the injector holes. By adding HTP, the freezing process of propyne would have been thus avoided. Nevertheless the use of a spark to ignite the mixture has been unsuccessful. This tempt is shown in Figure 28.

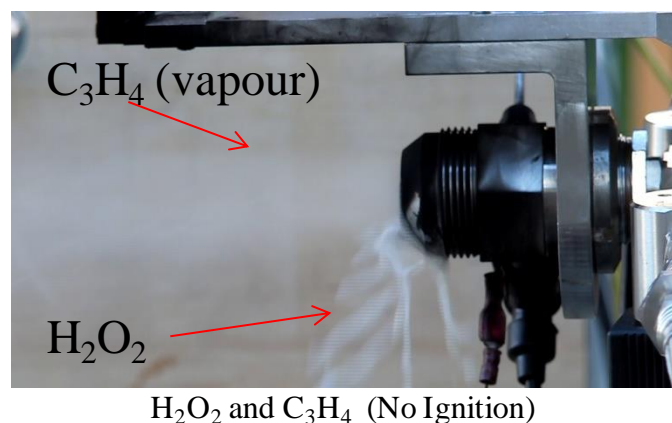


Figure 28. Contemporary injection of propyne and HTP with the injector PF1650+PA67-6-20-70. The tempt to ignite the mixture has been unsuccessful.

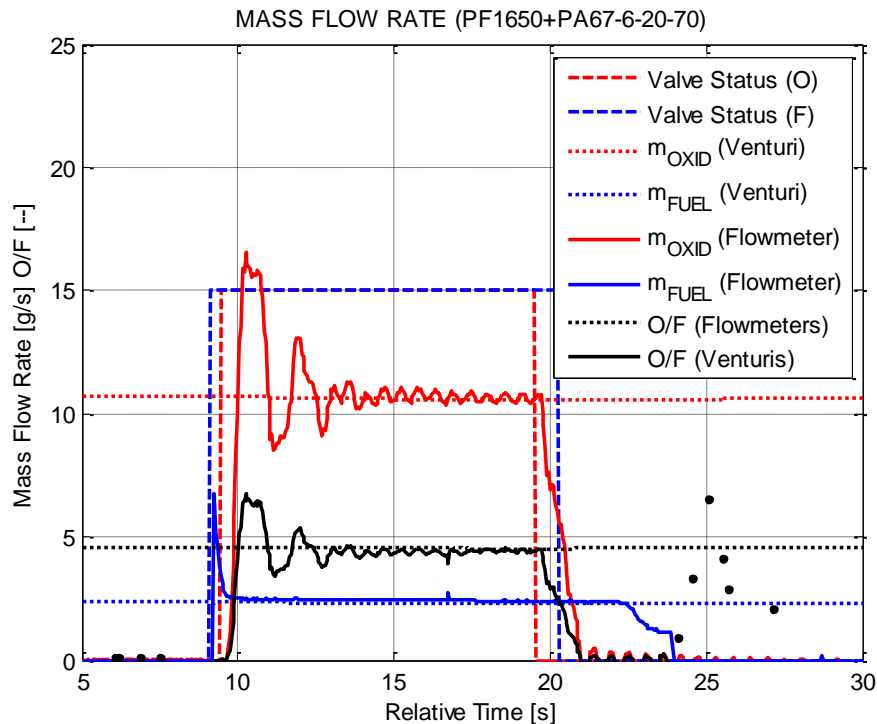


Figure 29. Spark plug as igniter of the liquid mixture test with PF1650+PA67-6-20-70: propellants mass flow rates and O/F ratio.

The time-evolution of the mass flow rates measured by the flowmeters confirms that the nominal O/F ratio has been reached during the experiment. However, the spark plug has not been able to ignite the highly atomized jet produced by the internal mix set-up coaxial injector.

5 EXPERIMENTAL CAMPAIGN ON THE BIPROPELLANT THRUSTER DEMONSTRATOR

5.1 Firing Tests with Liquid/Liquid Injection

All the firing tests with liquid/liquid injection have been performed using the metallic combustion chamber made of TZM. Figure 30 shows the set-up of the bipropellant thruster demonstrator before the firing tests. A surface thermocouple has been located on the external surface of the combustion chamber for monitoring its temperature in view of the calibration of the thermocamera.

According to the results of the ignition tests with liquid/liquid injection, the sequence of the test comprises the following phases:

- switch on of the spark plug;
- pulses of propyne until the ignition of the propyne;
- injection of propyne until the reaching of the steady-state of the decomposition of the fuel;
- injection of hydrogen peroxide for a maximum of 3-4 seconds due to material thrust chamber limitation;
- closing of the oxidizer valve;
- closing of the fuel valve;
- cooling of the bipropellant thruster demonstrator.

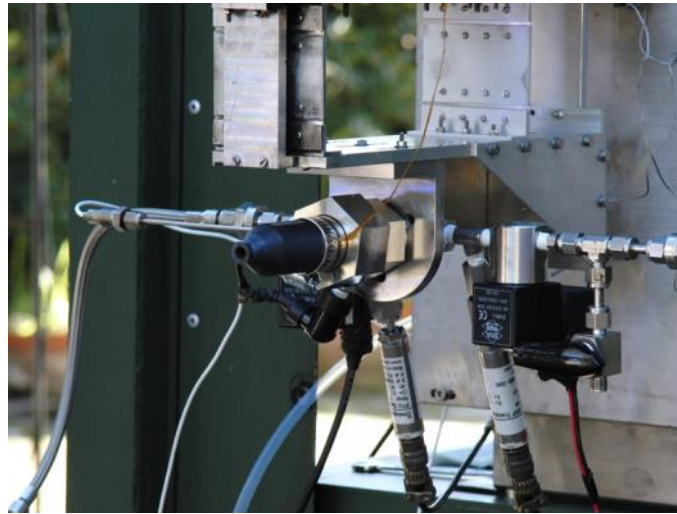
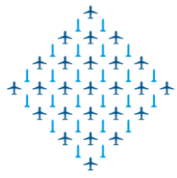


Figure 30. Bipropellant thruster demonstrator with the metallic (TZM) combustion chamber mounted on the thrust balance ready for the test with liquid/liquid injection.

Internal mix set-up: PF1650+PA67-6-20-70

The internal mix set up (PF1650+PA67-6-20-70) has proved to permit a good mixing and atomization of the propellants and, consequently, a uniform flame once the propellants have been ignited. Moreover, during the ignition test this configuration has shown some difficulties in the ignition of the propyne by the spark plug in such a way that multiple pulses have been necessary to start the decomposition reaction. However, the internal mix set-up (PF1650+PA67-6-20-70) has been finally chosen as the first configuration of liquid/liquid injection to be tested in the thruster demonstrator. As shown by the sequence of the experiment in Figure 31, after the injection of the propyne the spark plug has not been able to start the decomposition of the propyne.

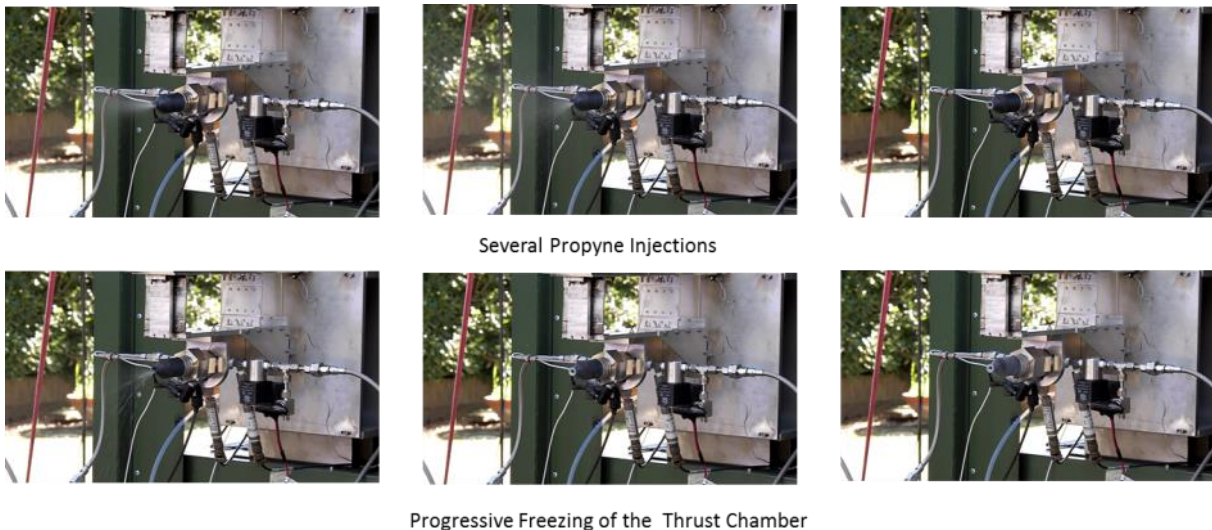


Figure 31. Sequence of different instants during the thruster firing (combustion chamber made of TZM) with internal mix set-up liquid/liquid injector.

After several attempts of igniting the propyne, due to the flashing of the fuel the pictures clearly shows the progressive freezing of the combustion chamber. The freezing of the thrust chamber is

confirmed by the drastic reduction of the external surface temperature of the combustion chamber reported in Figure 32.

Since the ignition of the propyne has not been occurred, the oxidizer firing valve has never been opened. Therefore, with respect to the test with only the injection manifold in which the spark plug has been able to begin the decomposition of propyne, the presence of the thrust chamber has resulted in unsuccessful experiments characterized by the absence of any ignition.

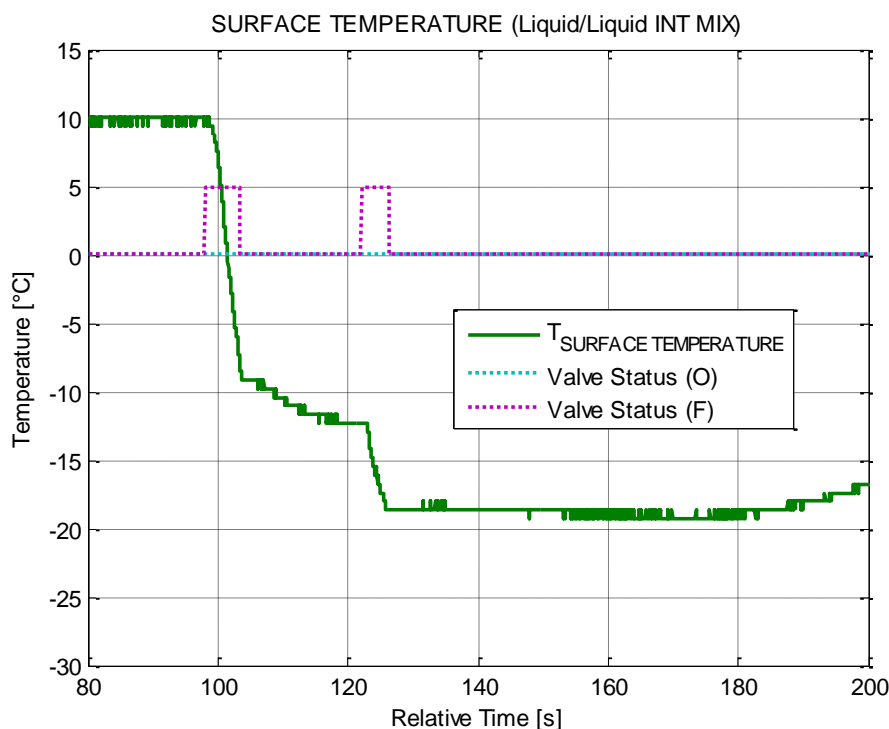


Figure 32. Liquid/liquid injection with internal mix set-up: temperature of the external surface of the thrust chamber.

External mix set-up: PF1650+PA64

With respect to the internal mix set-up, during the preliminary experiments the external mix set up (PF1650+PA64) has shown a jet pattern characterized by worst mixing and atomization efficiencies. Moreover, once ignited, the flame of the external mix set-up has been less uniform (see Figure 23 and Figure 26 for comparison) with more unreacted liquid hydrogen peroxide. However, this configuration has proved to be more prone and repeatable with respect to the ignition of the propyne with the spark plug. This happens mainly because the fuel jet is axially directed and it creates a recirculation zone of saturated propyne that is more likely to be ignited by the energy released by the spark plug. Figure 33 shows different instants during the firing with the external mix set-up liquid/liquid injector. Even in this case, the ignition of propyne has not been occurred. On the contrary, the thrust chamber has been frozen again by the flashing of the fuel. Due to the absence of the ignition of the fuel, the oxidizer has never been injected into the thrust chamber. The freezing of the thrust chamber is confirmed by the drastic reduction of the external surface temperature of the combustion chamber reported in Figure 34.

In this configuration the flashing of the fuel and the consequent decrease of the thrust chamber temperature has been less intense because the fuel jet does not directly impinge the chamber walls as in the case of the internal mix set-up. Even in this case, with respect to the test with only the injection manifold in which the spark plug has been able to begin the decomposition of propyne with

repeatability, the presence of the thrust chamber has resulted in unsuccessful experiments characterized by the absence of any ignition. Therefore, it has been not possible to measure the propulsive performance of the thruster demonstrator in this configuration. The main issue remains the spark plug and its capability of igniting the propyne.

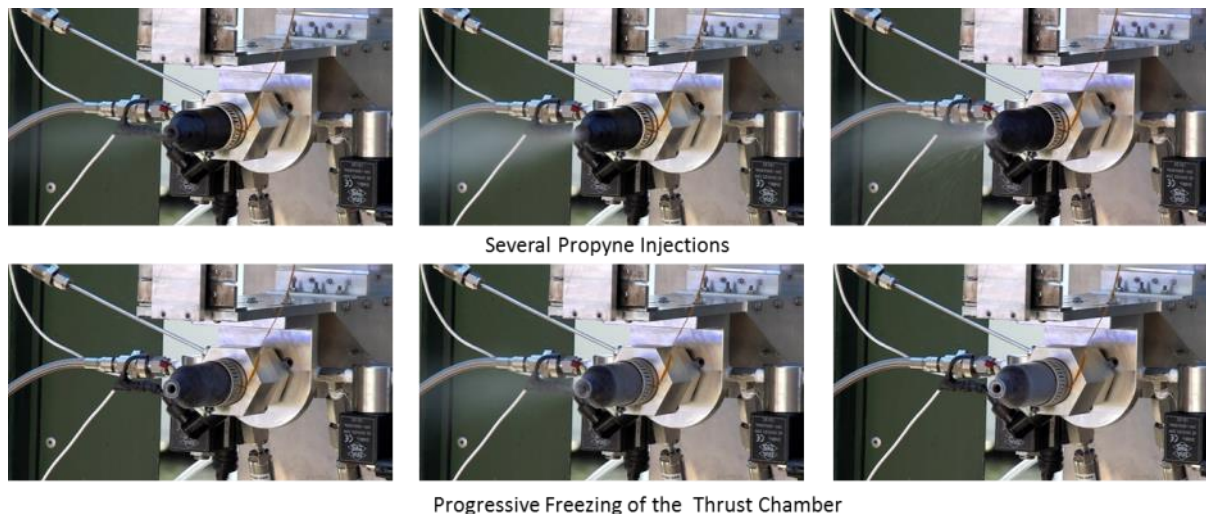


Figure 33. Sequence of different instants during the thruster firing (combustion chamber made of TZM) with external mix set-up liquid/liquid injector.

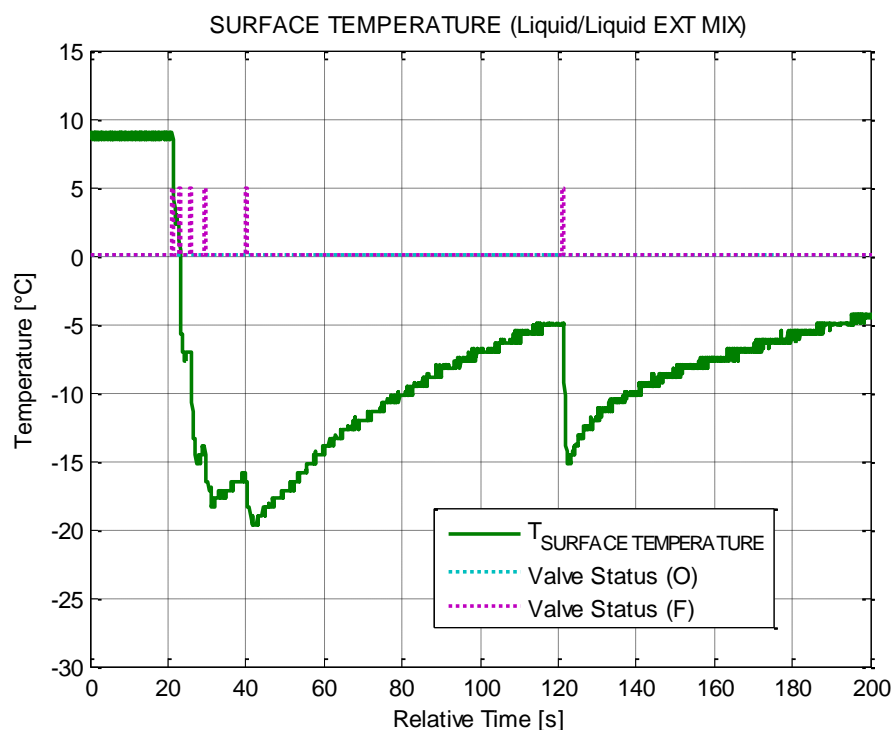


Figure 34. Liquid/liquid injection with external mix set-up: temperature of the external surface of the thrust chamber.

6 CONCLUSIONS

During the experimental campaign on the coaxial injectors, two injector configurations with satisfying jet patterns have been selected for the next tests with the bipropellant thruster demonstrator:

- external mix set-up PF1650+PA64 (inner fuel/outer oxidizer);
- internal mix set-up PF1650+PA67-6-20-70 (inner fuel/outer oxidizer).

The main results concerning the ignitability tests can be summarized as follows:

- the selected propellants (98% hydrogen peroxide and propyne) are not hypergolic;
- in case of liquid/liquid injection into the atmosphere, the selected propellants can be effectively ignited only if the spark plug is able to start the decomposition of the propyne. After the ignition of the propyne the resulting flame is capable of sustaining the combustion of propyne and hydrogen peroxide.

The lack of hypergolicity and the necessity of starting the decomposition of one of the propellants before the beginning of the combustion prove that propyne and hydrogen peroxide are not suitable for the implementation of the PulCheR concept with the tested ignition devices.

Despite the very promising ignition tests with the spark plug and the liquid/liquid injection, in the final configuration of the thruster demonstrator with the metallic combustion chamber, the spark plug has not been able to start the decomposition of the propyne and, consequently, the combustion of the propellants. The reason of this failure is still not clear and further investigations are required to identify a possible solution of the problem.

7 ACKNOWLEDGMENTS

The present work has been co-funded by the European Union Seventh Framework Programme (FP7/2007-2013) under grant agreement n°313271. SITAEL S.p.A. (formerly Alta S.p.A.) is proud to coordinate the project Consortium composed by leading companies in space technologies. Special tanks go to all the people of GMYS-Space.

8 REFERENCES

- [1] Pasini, A., Torre, L., Pace, G., Valentini, D., d'Agostino, L., 2013, "Pulsed Chemical Rocket with Green High Performance Propellants", *49th AIAA/ASME/SAE/ASEE Joint Propulsion Conference & Exhibit*, San Jose, California, 15-17 July, 2013. doi: 10.2514/6.2013-3756
- [2] Torre, L., Pasini, A., Pace, G., Valentini, D., d'Agostino, L., Siciliano, P. F., Lecardonnell, L., "PulCheR – Pulsed Chemical Rocket with Green High Performance Propellants: Project Overview", *Development Trends in Space Propulsion Systems*, Warsaw, 18-19 Oct. 2013.
- [3] Torre, L., Pasini, A., Pace, G., Valentini, D., d'Agostino, L., "PulCheR – Pulsed Chemical Rocket with Green High Performance Propellants: First Year Project Overview", *ESA Space Propulsion 2014 Conference*, Cologne, France, 19-22 May 2014.
- [4] Aneshansley, D. J., Eisner, T., "Biochemistry at 100°C: Explosive Secretory Discharge of Bombardier Beetles (*Brachinus*)", *Science*, 165:61-63 1, 1969.
- [5] Eisner, T., Aneshansley, D. J., "Spray Aiming in the Bombardier Beetle: Photographic Evidence", *Proc. Natl. Acad. Sci. USA*, Vol. 96, pp. 9705–9709, 1999.
- [6] Beheshti, N., McIntosh, A. C., "A biomimetic study of the explosive discharge of the bombardier beetle", *Int. J. Des. Nature* 1 61–9, 2007.
- [7] Talley, D. G., Coy, E. B., "Constant Volume Limit of Pulsed Propulsion for a Constant γ Ideal Gas", *AIAA 2000-3216*, *36th AIAA/ASME/SAE/ASEE Joint Propulsion Conference Huntsville, Alabama*, 17-19 July 2000.
- [8] Talley, D. G., Coy, E. B., "Constant Volume Limit of Pulsed Propulsion for a Constant γ Ideal Gas", *Journal of Propulsion and Power*, Vol. 18, No. 2, pp. 400-406, 2002.

- [9] Briggs, G. P., Milthorpe, J. F., "Strategic Propellant Choices for an Australian Medium Launch Vehicle", *7th Australian Space Science Conference*, Sydney, Australia, 2007.
- [10] Valentian, D., Sippel, M.; Gronland, T., Baker, A., van den Meulen, G., Fratacci, G.; Caramelli, F., "Green propellants options for launchers, manned capsules and interplanetary missions", *2nd International Conference on Green Propellants for Space Propulsion*, Chia Laguna, Italy, 2004.
- [11] European Chemicals Agency (ECHA), "Agreement of the Member State Committee on the Identification of Hydrazine as a Substance of Very High Concern", Adopted on 26 May 2011.
- [12] Valencia-Bell, F., Smith, M., "Replacement of Conventional Spacecraft Propellants with Green Propellants", *Space Propulsion Conference*, Bordeaux, France, May 7-10, 2012.
- [13] ESA Bulletin 154, May 2013, URL:
(http://www.esa.int/About_Us/ESA_Publications/ESA_Bulletin_154_May_2013).
- [14] Marshall, W. M., Deans, M. C., "Recommended Figures of Merit for Green Monopropellants", *49th AIAA/ASME/SAE/ASEE Joint Propulsion Conference & Exhibit*, San Jose, California, 15-17 July, 2013.
- [15] Bombelli, V., Simon, D., Marée, T. and Moerel, J.-L., "Economic Benefits of the use of Non-Toxic Monopropellants for Spacecraft Applications", *39th AIAA/ASME/SAE/ASEE Joint Propulsion Conference*, 20-23 July, Huntsville, AL, USA, 2003, AIAA paper n. 2003-4783. doi: 10.2514/6.2003-4783.
- [16] Pasini, A., Torre, L., Romeo, L., Cervone, A., d'Agostino, L., "Performance Characterization of Pellet Catalytic Beds for Hydrogen Peroxide Monopropellant Rockets", *AIAA Journal of Propulsion and Power*, Vol. 27, No. 2, pp. 428-436, Mar-Apr 2011.
- [17] Pasini, A., Torre, L., Romeo, L., Cervone, A., Masi, L., d'Agostino, L., "High Mass Flux Tests on Catalytic Beds for H₂O₂ Monopropellant Thruster", *ESA Space Propulsion 2010 Conference*, San Sebastian, Spain, May 2010.
- [18] Torre, L., Romeo, L., Pasini, A., Cervone, A., d'Agostino, L., "Propulsive Performance of a 100 ·m Pt/CexZr_{1-x}/Al₂O₃ Catalytic Bed", *47th AIAA/ASME/SAE/ASEE Joint Propulsion Conference*, San Diego, California, USA, August 2011.
- [19] Pasini, A., Torre, L., Romeo, L., Cervone, A., d'Agostino, L., "Testing and Characterization of a Hydrogen Peroxide Monopropellant Thruster", *AIAA Journal of Propulsion and Power*, Vol. 24, No. 3, pp. 507-515, May-Jun 2008.
- [20] Pasini, A., Torre, L., Pace, G., Valentini, D., "Stationary Propulsive Performance of a Green Monopropellant Thruster Demonstrator for the PulCheR Project", *ESA Space Propulsion 2014 Conference*, Cologne, France, 19-22 May 2014
- [21] Dolci, S., Belli Dell'Amico, D., Pasini, A., Torre, L., Pace, G., and Valentini, D., "Platinum Catalysts Development for 98% Hydrogen Peroxide Decomposition in Pulsed Monopropellant Thrusters", *Journal of Propulsion and Power*, Vol. 31, No. 4 (2015), pp. 1204-1216. doi: 10.2514/1.B35590
- [22] Goudon, JP, Yvart, P., Richard, B., Torre, L., Pasini, A., Martin, F., "Solid Modulated Propulsion for Space Exploration", *ESA Space Propulsion 2012 Conference*, Bordeaux, France, 7-10 May 2012.
- [23] Pasini, A., Pace, G., Torre, L., "A Light Unsaturated Hydrocarbon and Hydrogen Peroxide as Future Green Propellants for Bipropellant Thrusters", *51st AIAA/SAE/ASEE Joint Propulsion Conference*, Orlando, Florida, USA, 27-29 July 2015. (submitted for publication)
- [24] Happel, J., Marsel, C.J., 1953, "Acetylenic Compounds for Rocket Fuels", *New York University Bronx School of Engineering and Science*, Report Number: 0832820, December.